

**DETERMINATION OF WIND VELOCITY BY
DETECTING HELIUM BALLOON MOTION**

BY

NATAPORN KORPRASERTSAK

**A THESIS SUBMITTED IN PARTIAL FULFILLMENT OF THE
REQUIREMENTS FOR THE DEGREE OF MASTER OF SCIENCE
(ENGINEERING AND TECHNOLOGY)
SIRINDHORN INTERNATIONAL INSTITUTE OF TECHNOLOGY
THAMMASAT UNIVERSITY
ACADEMIC YEAR 2014**

**DETERMINATION OF WIND VELOCITY BY
DETECTING HELIUM BALLOON MOTION**

BY

NATAPORN KORPRASERTSAK

**A THESIS SUBMITTED IN PARTIAL FULFILLMENT OF THE
REQUIREMENTS FOR THE DEGREE OF MASTER OF SCIENCE
(ENGINEERING AND TECHNOLOGY)
SIRINDHORN INTERNATIONAL INSTITUTE OF TECHNOLOGY
THAMMASAT UNIVERSITY
ACADEMIC YEAR 2014**



DETERMINATION OF WIND VELOCITY BY DETECTING HELIUM
BALLOON MOTION

A Thesis Presented

By
NATAPORN KORPRASERTSAK

Submitted to
Sirindhorn International Institute of Technology
Thammasat University
In partial fulfillment of the requirements for the degree of
MASTER OF SCIENCE (ENGINEERING AND TECHNOLOGY)

Approved as to style and content by

Advisor and Chairperson of Thesis Committee



(Prof. Thananchai Leephakpreeda, Ph.D.)

Committee Member



(Asst. Prof. Anotai Suksangpanomrung, Ph.D.)

Committee Member and

Chairperson of Examination Committee



(Assoc. Prof. Supachart Chungpaibulpatana, D.Eng)

MAY 2015

Abstract

[DETERMINATION OF WIND VELOCITY BY DETECTING HELIUM
BALLOON MOTION]

by

NATAPORN KORPRASERTSAK

[Mechanical Engineering: Bachelor, Sirindhorn International Institute of Technology,
2012]

Wind Velocity Measurement is the major key of research and development for wind mill electricity production. The most common method of measurement is set up by install the measuring device on the pillar at the desire height, technically at 40 to 100 meters of height. The measurement of wind velocity can be done by study and analyst the characteristic of wind using the principle of aerodynamic. The sample balloon filled with helium gas can be float at the desired height that can control by the length of rope. At the end of the rope will be connected with the rotating device. The rotating device is design to face in the same direction of wind all the time. Wind velocity is derived by the reaction from helium balloon using principle of aerodynamic. The calculation is done by mathematic model. The wind cause drag force that lead to dynamic equilibrium of balloon motion. By knowing buoyancy, gravity, rope tension and the angle between rope and vertical line of helium balloon, the wind velocity at the specific height of balloon can be calculated by motion equation and drag equation. The measurement also apply wind profile power law to adjust wind velocity for varies height. This measurement model done by experiment and develop compare to practical field measuring device. The experiment result show that the helium balloon have potential to measure wind velocity as same as the pillar type.

Keywords: wind measurement, helium balloon, dynamics interpretation, wind profile power law.

Acknowledgement

The author would like to express my sincere thanks to my thesis advisor, Prof. Dr. Thananchai Leephakpreeda for his invaluable advice and continuous support of this research. Furthermore, the author also sincerely thank the rest of my thesis committee: Assoc. Dr. Supachart Chungpaibulpatana and Asst. Prof. Dr. Anotai Suksangpanomrung for their encouragement, insightful comments, and hard questions. In addition, the author is grateful for the SIIT mechanical technician: Mr. Nikhom Meedet and Mr. Manatchai Srimatra, who helped design and build the device and supply so many tools or equipment for this project. Finally, My sincere thanks also goes to staff of Pilot Plant Development and Training Institute, King Mongkut's University of Technology Thonburi, who helped to support the place to test the measurement device and give the information of wind profiles.

Table of Contents

Chapter	Title	Page
	Signature Page	i
	Acknowledgement	ii
	Abstract	iii
	Table of Contents	iv
	List of Figures	vi
	List of Tables	viii
1	Introduction	1
2	Literature Review	4
	2.1 Wind vane	4
	2.2 Anemometer	5
	2.3 Wind measurement with the Multiple Antenna Profiler (MAPR)	5
	2.4 Wind measurement with Doppler Lidar	7
3	Methodology	8
	5.1 Determination of wind direction	9
	5.2 Fluid mechanics of a helium balloon in the atmosphere	11
	5.2 Determination of wind speed	14
	5.2 Determination of wind speed in y-axis	17
4	Experiment Setup and Design of Mechanism	18
	4.1 Experiment Setup	18
	4.2 Modeling and design of mechanism	20

4.2.1 Project Device Assembly	22
4.2.1 Project Device Installation	23
5 Results and Discussion	24
6 Conclusions	32
4.1 Conclusions	32
4.2 Future work	33
References	34
Appendices	37
Appendix A	38
Appendix B	52
Appendix C	61

List of Figures

Figures	Page
1.1 Wind data at a height of 60 m: (a) speed and (b) direction	1
2.1 Wind vane	4
2.2 Anemometer	5
2.3 MAPR with clutter screen	6
2.4 MAPR with four vertically pointing	6
2.5 Doppler Lidar	7
3.1 Installation of helium balloon for wind measurement	8
3.2 Motion analysis of helium balloon	9
3.3 Free body diagram of helium balloon in atmosphere	12
3.4 Trajectory of helium balloon with wind	14
3.5 Determination of wind direction and wind magnitude	15
4.1 Experimental setup of wind measurement system using helium balloon near wind mast	18
4.2 Diagram of data acquisition system for balloon measurements	19
4.3 A part of mechanism to measure wind direction	20
4.4 A component in direction part	20
4.5 A part of mechanism to measure wind speed	21
4.6 Project device assembly (1)	22
5.1 Motions of helium balloon at constant wind speed: (a) 2 m/s, (b) 4 m/s, (c) 6 m/s, and (d) 8 m/s	25
5.2 Simulated results under real wind blow: (a) actual wind speed, (b) height of helium balloon, and (c) swing angle	26
5.3 Plots of simulated results and measured data of wind speed against time at height of 60 m	27
5.4 Determination of ground friction coefficient α	29
5.5 Determination of ground friction coefficient by using two sets of measurement device.	29
5.6 Plots of experimental results reported in one day: (a) wind speed against time and (b) wind rose diagram of wind direction	30



List of Tables

Tables	Page
5.1 Numerical values of parameters used in simulation	24
5.2 Numerical values of parameters used in experiment	28
5.3 Examples of measured data and determined results	28



Chapter 1

Introduction

Measurements of elevated wind speeds in areas with expected potential for the installation of wind farms are highly important for the evaluation of electricity generation from wind power and for the development of wind farms of appropriate sizes (Barthelmie et al., 2005; Oh et al., 2012; Chen et al., 2013; Song et al., 2014). Generally wind speeds will be measured continuously, both the variables of wind speed and direction in a certain time period. The example in Figure 1.1 displays the statistical data of the frequency of wind variables in forms of a wind speed data graph and a chart of directions of winds higher than 60 meters, of which data details of wind speed and direction will explain the evaluation for the determination of possible windmill sizes and the placement of windmills for electricity generation to be efficient according to the terrain conditions and wind direction in those areas.

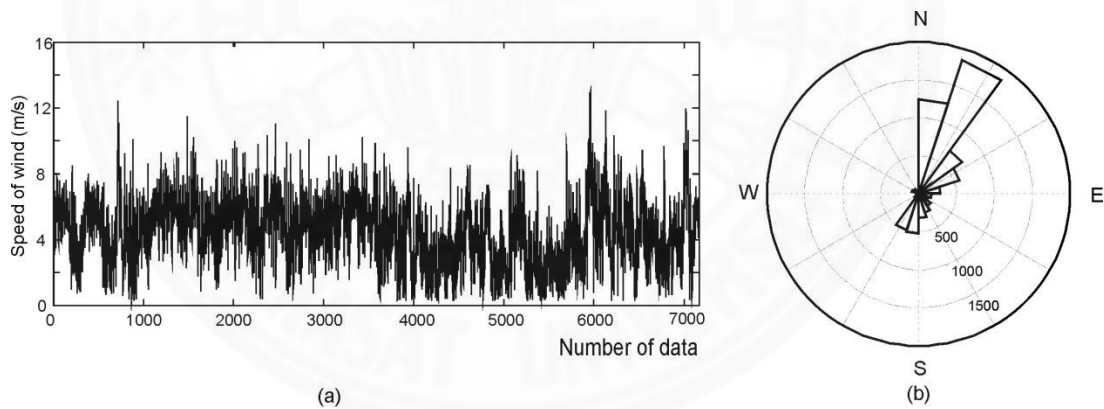


Figure 1.1 Wind data at a height of 60 m: (a) speed and (b) direction

The equipment used for measuring wind speed will need to be installed on a pole with a height of 40-100 meters at the site of study that may be comprised of data loggers, a data transfer system via GSM/GPRS networks, a power source, other additional equipment, and an anemometer to measure both wind speed and direction, of which equipment are very important for measuring wind speeds. There are many

types of anemometers. The type of anemometer that is generally used are propeller-based anemometers such as the three-cup anemometer or propeller anemometer, which are the fundamental instruments for measuring wind speed; these measuring instruments are often used with wind vanes to measure wind direction where these measuring instruments use little electric power and often have systems to store electric energy with the use of sufficient solar energy. In addition to propeller-based anemometers, there are also ultrasonic anemometers that have the ability to measure wind speed and direction together, but they require a large power source as an energy source (Emeis, 2010); there must be experts to install these anemometers in appropriate locations on wind-mast and they have high costs in part of the construction, installation, and maintenance of the measurement poles.

As for alternative options for measuring wind speed without installations on wind-mast, other techniques based on the foundations of the detection of objects in the atmosphere can be used, with the transmission of radio waves or lasers to the atmosphere to observe wind speed and direction. Examples such as the Multiple Antenna Profiler (MAPR) use radio waves to track movements in the atmosphere (Brown et al., 1999; Lataitis et al., 2005). Additionally, laser detection is used in Laser Imaging Detection and Ranging (LIDAR), which is a wind speed measurement system via laser transmission into the atmosphere and the reception of scattered light based on the speed of aerosols (Wu et al., 2012), but equipment costs are high. Difficult installation and maintenance procedures, especially in remote sites are thus limitations for their uses in practical implementations in the present. Additionally, the signals transmitted can be absorbed by mist and other substances, which can reduce the efficiency of measurements.

This study was for the presentation of new alternatives for low cost wind speed measurements by studying the movement of helium balloons that float in the atmosphere at heights where measurements were intended to be done, where it was discovered that the floatation of helium balloons follow air current profiles (Bañuelos-Ruedas et al., 2011). Helium balloons were held to specially designed rotating arm mechanisms through thick ropes. While the rotating arm mechanism was anchored to the ground, the helium balloon was set to float up to the desired height instead of building a wind-mast at that height. This rotating arm mechanism has been designed

such that it will stop rotating once the rotating arm points in the same direction as the air current. Because the rope will pull the endpoint of the rotating arm and cause a moment around that axis, rope tension will act and cause the rotating arm's moment to be zero only when the rotating arm points in the same direction as the wind while the air's blowing may cause resistant drag forces on the helium balloon, which can be used to calculate wind speed (Bertin and Smith, 1988).



Chapter 2

Literature Review

In the measurement of wind velocity, the method which is mostly be used are using anemometer and wind vane. It is used for measuring the wind velocity and wind direction to bring the data or information to consider that the wind profile in the area is appropriate or not to build wind turbines to produce wind energy. There are other research which are using various method or technology to measure the wind profile.

2.1 Wind vane

Wind vane as shown in Figure 2.1 utilizes the principle of drag force exerted by wind (Pratt, 2008). When the wind flow through the measurement device perpendicularly, the maximum drag force occurs at the tail part of the device where the drag area is highest. The wind drag force pushes the device to rotate around the shaft until the tail is parallel to the wind direction where the drag area is lowest. The wind direction can be determined from those principle.



Figure 2.1 Wind vane (Pratt, 2008)

2.2 Anemometer

There are various type of anemometer such as Cup Anemometer, Windmill anemometer, Hot wire Anemometer, Ultrasonic Anemometer, etc. However, the popular anemometer are typically windmill type or three-cup type as shown in Figure 2.2 which consists of three branches connecting to each other at the middle. Also, the shaft links the middle part to the bottom part. When the windmill rotates, the electric current is generated that makes the needle at the dial point to detect wind speed (Bellis, 2015).

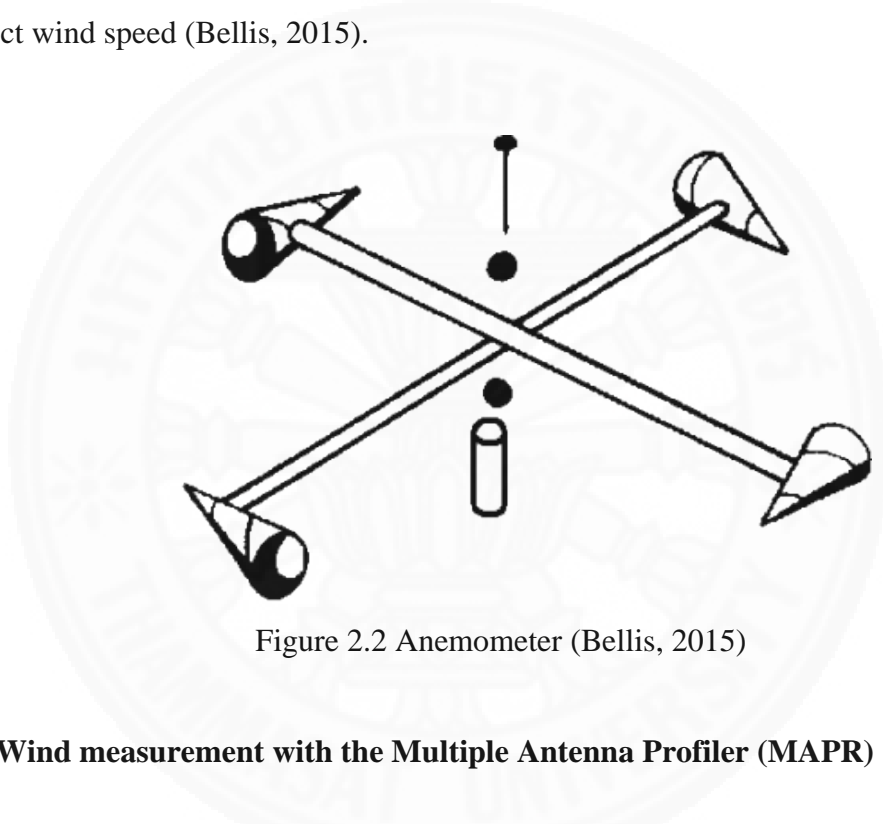


Figure 2.2 Anemometer (Bellis, 2015)

2.3 Wind measurement with the Multiple Antenna Profiler (MAPR)

Multiple Antenna Profiler (MAPR) as shown in Figure 2.3 generally uses in Integrated Sounding System. MAPR utilizes the technique of spaced antenna to determine wind profiles (Cohn et al., 2001). MAPR method is based on the mechanism of air movement and small particle movement. It uses technique called Spaced Antenna Winds to determine wind speed rapidly by the movement of air flow. After that, the air movement will be tracked and send the signal back to the receiver antennas for determining wind speed. The radar is designed for determining wind speed faster than another typed of wind measurement. The radar has four vertically pointing as shown in Figure 2.4 so that it is able to detect moving particle rapidly.



Figure 2.3 MAPR with clutter screen (Cohn et al., 2001)

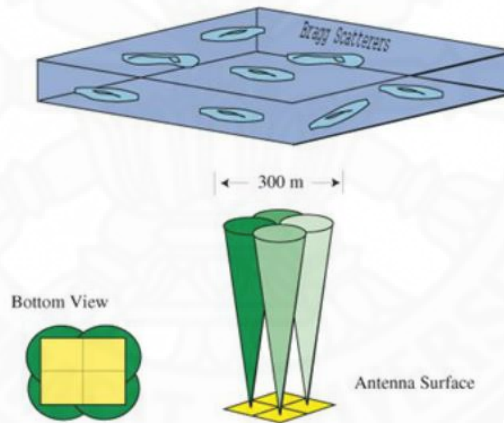


Figure 2.4 MAPR with four vertically pointing (Cohn et al., 2001)

2.4 Wind measurement with Doppler Lidar

"Lidar" or "Laser Imaging Detection And Ranging" or "Light Detection And Ranging" is the measurement device based on the principle of lighting wave (Shen et al., 2008). it can measure the speed of moving object. The Doppler Lidar as shown in Figure 2.5 works by sending laser beam into the air and it will be reflected by the dust particle flowing through the light (the dust particle has diameter of 10 microns). The signal moving through laser is taken to compute wind speed and wind direction.

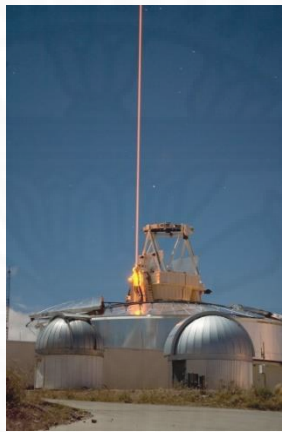


Figure 2.5 Doppler Lidar (Shen et al., 2008)

All technology or methods of other researches are designed to measure the wind profile or measure the wind speed and wind direction in different way. All of above use a high technology to generate the data of wind profiles. In a part of the results, the data of wind speed and wind direction are almost precisions, because they use the principle of laser or radars that are very accurate.

Chapter 3

Methodology

The wind velocity is determined by interpreting motions of the helium-balloon at the height where the wind velocity is to be measured. The helium balloon is installed at the desired height where it is pulled by a cord of corresponding length. The end of the cord is tied to a specially-designed holding mechanism of a rotating arm, which always leads to direction of wind as depicted in Figure 3.1. For wind speed, aerodynamic performance of the helium balloon is investigated. The simulation of this theory were shown in Appendix C.

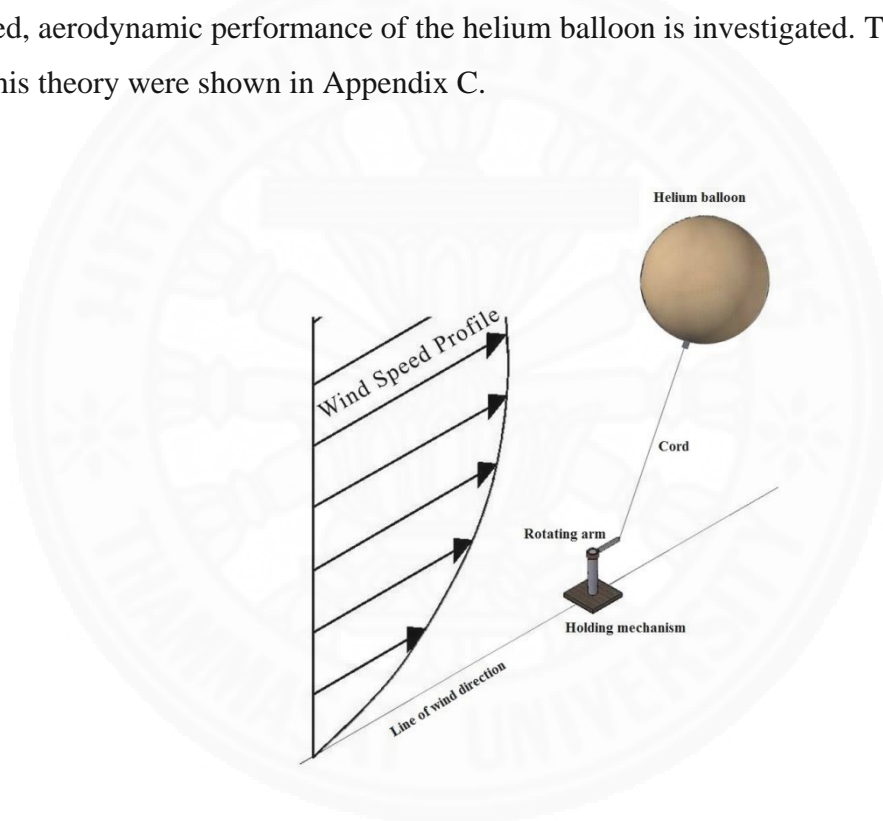


Figure 3.1 Installation of helium balloon for wind measurement

3.1 Determination of wind direction

A mechanism of a rotating arm is designed to swing a cord leading to the direction of wind as shown in Figure 3.2. The tension of the cord can be defined as:

$$\vec{T} = F_t \vec{u}_t \quad (3.1)$$

Where \vec{T} is the vector of the tension in the cord,

F_t is the magnitude of tension in the cord, and

\vec{u}_t is the unit vector along the cord pointing from the rotating point to the helium balloon.

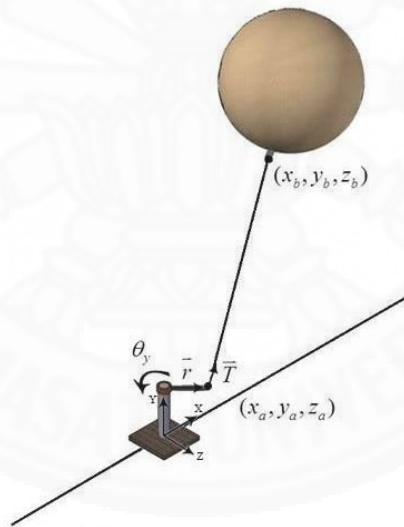


Figure 3.2 Motion analysis of helium balloon

The unit vector of the tension can be expressed as:

$$\vec{u}_t = \frac{1}{L} [(x_b - x_a)\vec{u}_x + (y_b - y_a)\vec{u}_y + (z_b - z_a)\vec{u}_z] \quad (3.2)$$

Where (x_b, y_b, z_b) is the coordinate where the cord is attached to the helium balloon,
 (x_a, y_a, z_a) is the coordinate where the cord is attached to one end of the rotating

arm,

L is the length of the cord,

\vec{u}_x is the unit vector in the direction of x-axis,

\vec{u}_y is the unit vector in the direction of y-axis, and

\vec{u}_z is the unit vector in the direction of z-axis.

The tension in the cord can be expressed as:

$$(\vec{r} \times \vec{T}) \cdot \vec{u}_y = I_y \ddot{\theta}_y \quad (3.3)$$

Where \vec{r} is the position vector of the rotating arm pointing from the rotating point to the ending point of the rotating arm,

I_y is the moment of inertia about the y axis, and

$\ddot{\theta}_y$ is the angular acceleration of the rotating arm about the y axis.

By manipulating (3.3), the moment can be obtained as:

$$\frac{F_t}{L} \left[x_a(x_b - x_a) \left[\left(\frac{z_b - z_a}{x_b - x_a} \right) - \frac{z_a}{x_a} \right] \right] = I_y \ddot{\theta}_y \quad (3.4)$$

When the slope of the cord is $\left(\frac{z_b - z_a}{x_b - x_a} \right)$, and the slope of the rotating arm is $\left(\frac{z_a}{x_a} \right)$, In horizontal plane there are equal. Therefore, the moment about y-axis is zero.

That means the rotating arm will stop rotating once it points in the same direction as the air current. So, the rotating angle θ_y can be used to measure the wind direction.

3.2 Fluid mechanics of a helium balloon in the atmosphere

The movement or motion of a helium balloon and the flow of air around the helium balloon surface are caused by friction at the surface of the helium balloon. A partial vacuum is occurred behind the helium balloon or opposite the strike force of air. Therefore, the drag force is influenced to determine the wind speed (Bertin and Smith, 1988; Leephakpreeda, 2010) and can be defined as:

$$F_d = \frac{1}{2} c_d A \rho (v - v_b)^2 \quad (3.5)$$

Where F_d is the drag force,

c_d is the drag coefficient as discussed in the Appendix,

A is the cross-sectional area of the helium balloon,

ρ is the density of the air, v is the wind speed, and

v_b is the speed of the helium balloon in the direction of wind.

When the wind speed is zero or there is no air around the helium balloon, the helium balloon will float up vertically in the atmosphere by the helium gas in the balloon. When there is wind speed occurred to the helium balloon, it will move and change the position. The motion or the movement of the helium balloon is caused by vertical and horizontal forces are shown in Figure 3.3. The balance force can be determined by:

For y-axis:

$$F_b - F_t \cos \theta - mg = m\ddot{y} \quad (3.6)$$

For x-axis:

$$F_d - F_t \sin \theta = m\ddot{x} \quad (3.7)$$

Where F_b is the buoyancy force,

F_d is the drag force,

m is the total mass of the helium balloon,

θ is the swing angle between the cord and the vertical line,

g is the gravitational acceleration,

\ddot{x} is the acceleration in the x axis, and

\ddot{y} is the acceleration in the y axis.

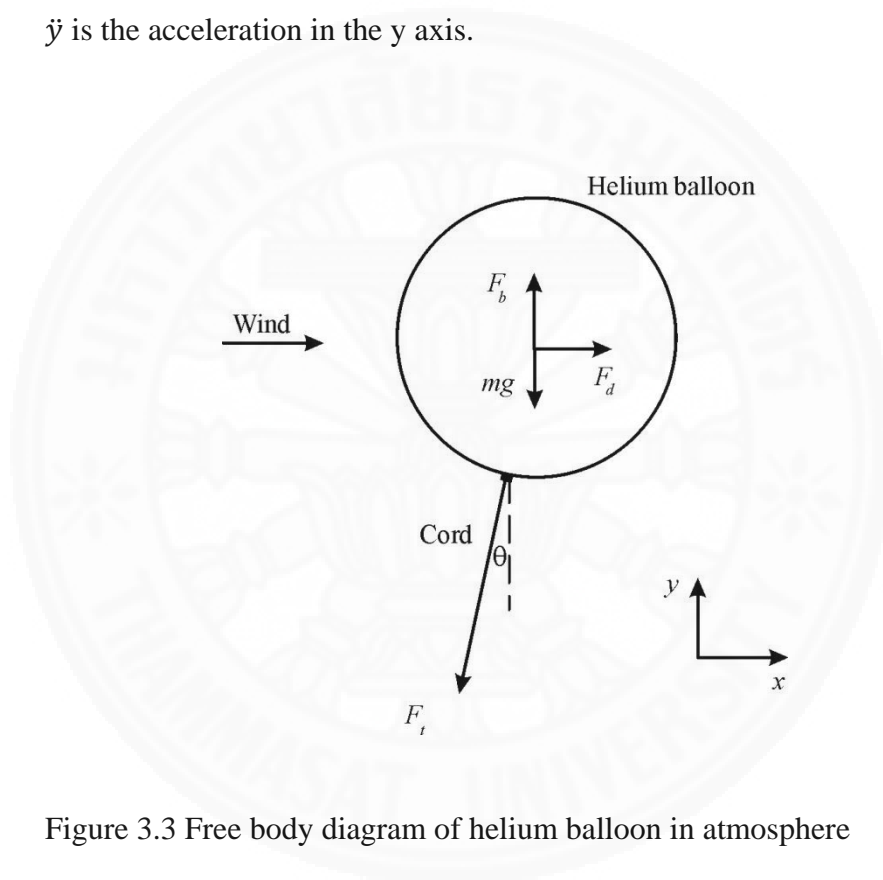


Figure 3.3 Free body diagram of helium balloon in atmosphere

The mass of helium gas and mass of balloon can be expressed as:

$$m = m_b + m_h \quad (3.8)$$

Where m_b is the mass of the balloon,

m_h is the mass of the helium gas.

The mass of the balloon can be weighed while the mass of helium can be determined by:

$$m_h = \rho_h V_b \quad (3.9)$$

Where ρ_h is the density of helium gas,
 V_b is the volume of the helium balloon.

The buoyancy force that caused by the weight of air which is replaced by helium gas can be calculated as:

$$F_b = \rho V_b g \quad (3.10)$$

To make this operating work, the buoyancy force of the helium balloon must be greater than the total weight of the balloon and helium gas in order to make the balloon float up in the atmosphere. The rope is attached to the balloon and swing arm is the desired height.

3.3 Determination of wind speed

As the helium balloon is connected with the rope to the holding mechanism, the helium balloon is moving as the circular path as shown in Figure 3.4. The position of the helium balloon in the horizontal axis can be determined as:

$$x = x_a + (L + R) \sin \theta \quad (3.11)$$

Where R is the radius of the helium balloon.

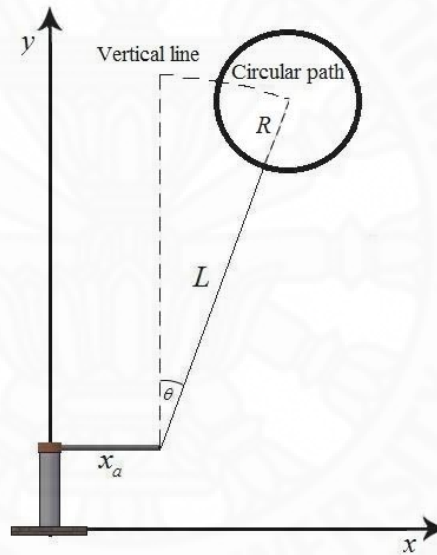


Figure 3.4 Trajectory of helium balloon with wind

When the helium balloon is moving, the acceleration of movement is occurred. The acceleration and speed of the helium balloon can be calculated by the positions in various times:

$$\ddot{x} = \frac{x(t) - 2x(t - \Delta t) + x(t - 2\Delta t)}{(\Delta t)^2} \quad (3.12)$$

And

$$v_b = \frac{x(t) - x(t - 2\Delta t)}{2(\Delta t)} \quad (3.13)$$

Where Δt is the sampling time,

$x(t)$ is the positions of the helium balloon at times t ,

$x(t - \Delta t)$ is the positions of the helium balloon at times $(t - \Delta t)$, and

$x(t - 2\Delta t)$ is the positions of the helium balloon at times $(t - 2\Delta t)$.

The drag force from (3.7) due to the wind speed can be determined by:

$$F_d = m\ddot{x} + F_t \sin \theta \quad (3.14)$$

Therefore, the wind speed is determined by:

$$v = \sqrt{\frac{F_d}{0.5\rho c_d A}} + v_b \quad (3.15)$$

It be concluded that the wind direction is determined by the rotating angle of the holding mechanism, while the wind speed can be determined by the tension of the pulling cord and swing angle as concluded in diagram Figure 3.5.

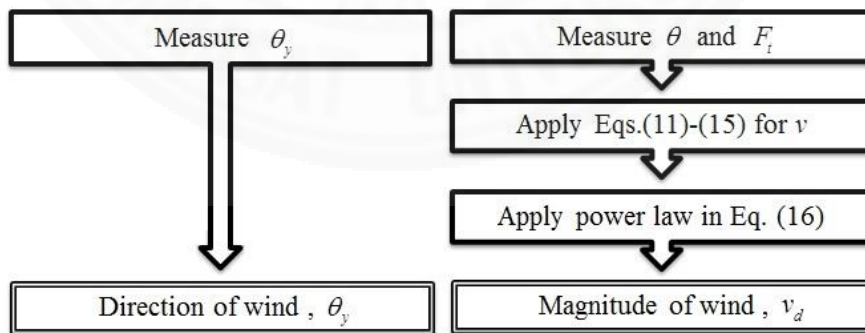


Figure 3.5 Determination of wind direction and wind magnitude

According to the helium balloon moving as the circular path, therefore the position of the helium balloon is always lower than the desired height. So, it had to apply wind profile power law in order to determine the wind speed at the desired height. It can be define as:

$$v_d = v \left(\frac{y_d}{y} \right)^\alpha \quad (3.16)$$

Where v_d is the wind speed, which is determined at a desired height y_d and v is the wind speed, which is determined at the balloon height y , and α is the ground friction coefficient which is dependent on geographical and atmospheric factors (Klink, 2007).

The one-seventh-power law (Mukund, 1999) is commonly used. Furthermore, the ground friction coefficient can be determined by the information of wind speed in two different levels. It can be define as:

$$\log \left(\frac{v_d}{v} \right) = \alpha \log \left(\frac{y_d}{y} \right) \quad (3.17)$$

The value of the ground friction coefficient for this project is determined by using the two sets of mechanism device in order to record the wind speed of two different levels.

3.4 Determination of wind speed in y-axis

As the helium balloon is moving as the circular path as shown in Figure 3.4. The position of the helium balloon in the vertical axis can be determined as:

$$y = \sqrt{L^2 - x^2} \quad (3.11)$$

The acceleration and speed of the helium balloon in y-axis can be calculated by the positions in various times:

$$\ddot{y} = \frac{y(t) - 2y(t - \Delta t) + y(t - 2\Delta t)}{(\Delta t)^2} \quad (3.12)$$

And

$$v_{by} = \frac{y(t) - y(t - 2\Delta t)}{2(\Delta t)} \quad (3.13)$$

The drag force from (3.6) due to the wind speed in vertical axis can be determined by:

$$F_{dy} = m\ddot{y} + mg - F_b + F_g + F_t \cos\theta \quad (3.14)$$

The equation for determining the vertical wind speed can be written as:

$$v_y = \sqrt{\frac{F_{dy}}{0.5\rho c_d A}} + v_{by} \quad (3.18)$$

Chapter 4

Experiment Setup and Design of Mechanism

4.1 Experiment Setup

This measurement device has two main functions. The former is measurement of wind direction and the latter is measurement of wind speed.

In this experiment, the anemometers were installed on a mast at various height. The wind profile of 40 heights will be taken to be compared with the data obtained from this device. The wind mast is consisted of three-cup anemometer of NRG#40C has a measuring range of 1-96 m/s with accuracy of 0.1 m/s (5-25 m/s) while the wind vane of NRG#200P has 360° continuous rotation with potentiometer linearity within 1%.

First, the base is installed on smooth ground surface at open area. The distance between the base and the wind mast is 120 meters approximately. The base is weighted in order to prevent the device from lifting up due to very height tension of balloon. After that the device is assembled to the base and set the angle of rotary potentiometer to 0° as north. Then, a balloon of a 3-m diameter is filled with helium gas and connect with the rope length 38.25 meter (height of swing arm to ground is 0.25 meter and radius of helium balloon is 1.5 meter) as shown in Figure 4.1.



Figure 4.1 Experimental setup of wind measurement system using helium balloon near wind mast

Finally, measurement data of wind speed and wind direction are acquired and recorded by a data acquisition system as presented in Figure 4.2. There are three potentiometers, which are one linear potentiometer and two rotary potentiometers. One linear and one rotary potentiometer are used to generate voltage signals of tension force and swing angle of the vertical line respectively for measuring the wind speed. Another rotary potentiometer is used to generate the voltage signals of an angular position of the rotating arm for measuring the wind direction.

The experiment data is recorded for 1 day or 24 hours. After that the voltage signal data obtained from the three potentiometer was taken to calculate wind direction and wind speed. Then the final data will be compared with the wind mast data at the same measuring time.

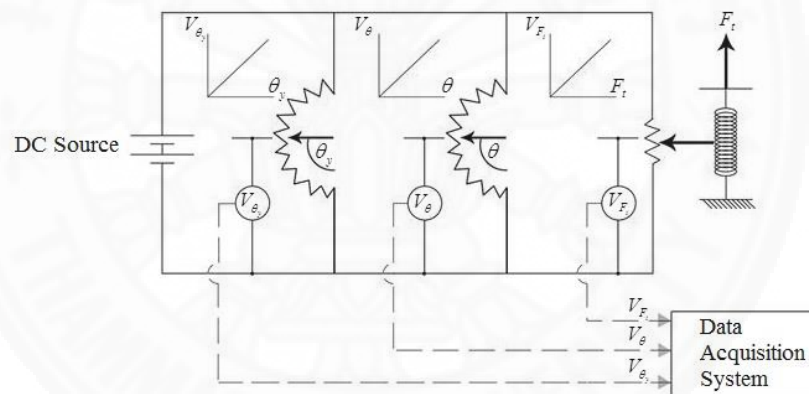


Figure 4.2 Diagram of data acquisition system for balloon measurements

4.2 Modeling and design of mechanism

The design of the mechanism is divided into two parts, first is the direction part and second is the velocity part.

For direction part as shown in Figure 4.3, the main component is the beam with the baring and the rotary potentiometer located at the center as shown in Figure 4.4. This entire part is covered by the cap with the swing arm connected at the top.

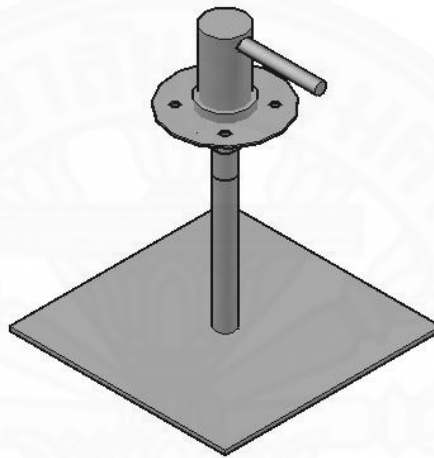


Figure 4.3 A part of mechanism to measure wind direction

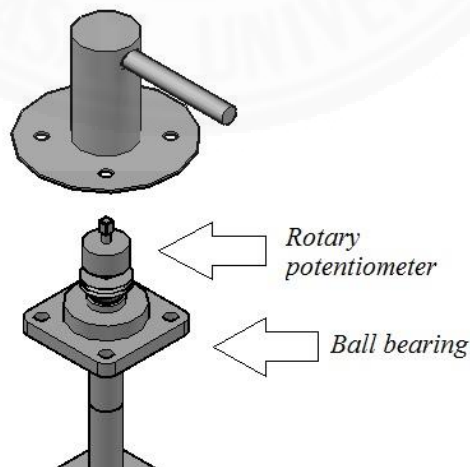


Figure 4.4 A component in direction part

The mechanism is that when the cap with the swing arm rotates, the shaft of rotary potentiometer will rotate according to the cap's rotation. The resistance value will be converted to the wind direction value.

For velocity part, the component is the beam for pulling the rope connected to the balloon. The beam is connected to the spring in purpose to determine the rope's tension. For this part, two types of potentiometer are used, the rotary potentiometer is used to determine the value of angle and the linear potentiometer working with the spring is used to measure the rope's tension. The beam is able to swing in vertical direction and the data will be recorded as angle. Figure 4.5 shows the part of mechanism to measure wind speed. The dimension of mechanism device are shown in the Appendix A.

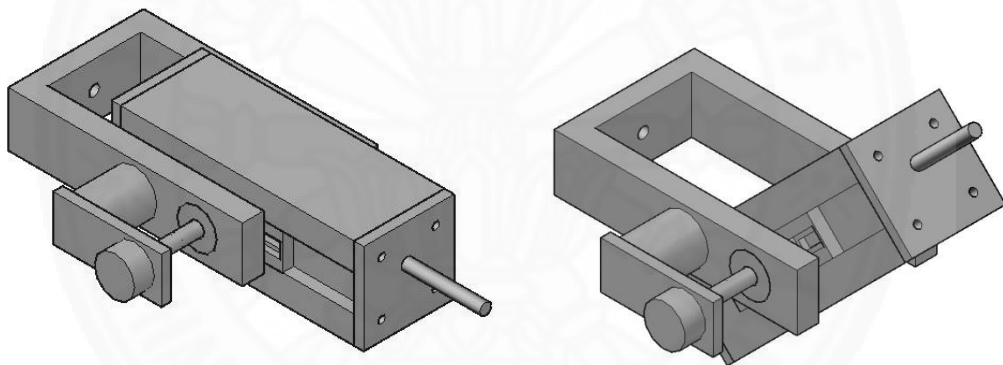


Figure 4.5 A part of mechanism to measure wind speed

4.2.1 Project Device Assembly

- Insert the pole through the hole of housing bearing and lock them to each other as shown in Figure 4.6 (a).
- Cover the housing bearing with the skirt as shown in Figure 4.6 (b).
- Assemble the potentiometer following the figure as shown in Figure 4.6 (c).
- Assemble the completed potentiometer set with the pole by braiding them to each other as shown in Figure 4.6 (d).
- Cover the completed potentiometer set with the cap and insert 4 bolts to bind the cap with the skirt as shown in Figure 4.6 (e).
- Insert, by braiding, the swing arm into the hole on the top of the cap as shown in Figure 4.6 (f).
- Connect the velocity part to the swing arm as shown in Figure 4.6 (g).



(a)



(b)



(c)



(d)



(e)



(f)

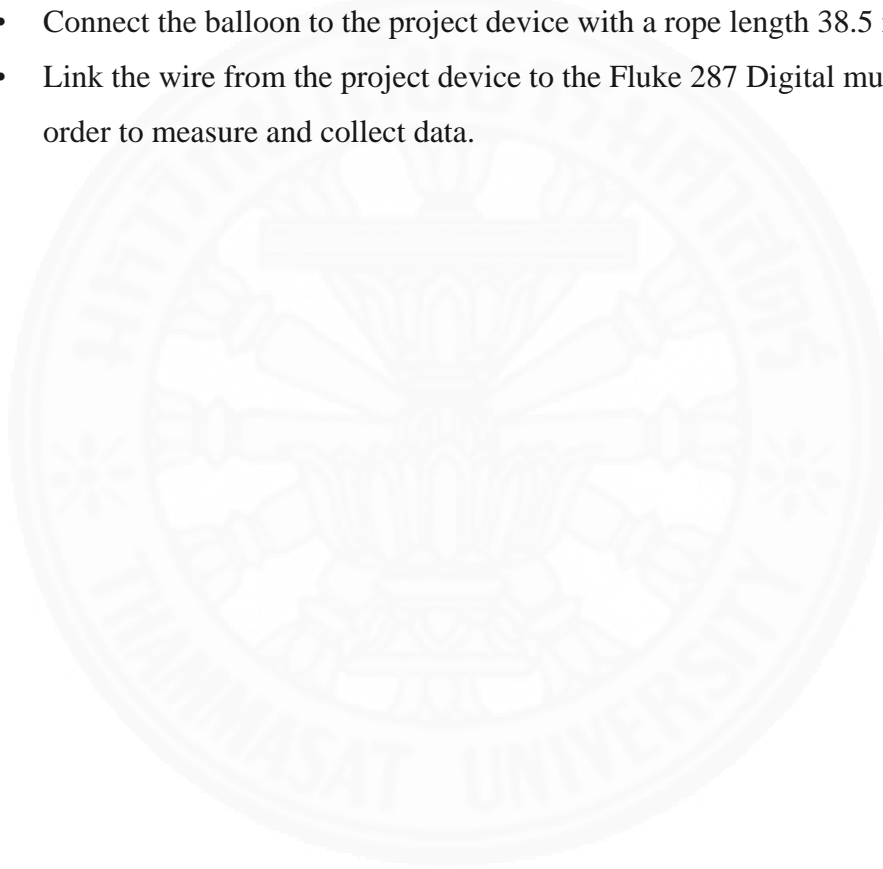


(g)

Figure 4.6 Project device assembly

4.2.2 Project Device Installation

- Wind vane and anemometer are installed at a height of 40 m.
- Install the project device on the ground (Flat surface) by the distance between the project device and Wind vane and anemometer is approximately 120 meters.
- Fill a plastic balloon of a 3-m diameter with helium gas.
- Connect the balloon to the project device with a rope length 38.5 meters.
- Link the wire from the project device to the Fluke 287 Digital multi meter in order to measure and collect data.



Chapter 5

Results and Discussion

In this chapter the solutions obtained from numerical modeling and the experimental results of the workings of the measurement device will be presented to explain the physical workings of helium balloon anemometer's system, in which wind speeds were calculated from some variables in the mathematical model of the aerodynamic behavior within the movement of the helium balloons.

In studies with numerical models, balloons with a diameter of 3 meters were used and held with rope at a height of 60 meters. All numerical parameter values that were used in the numerical model were said in chapter 5 and determined in Table 5.1

Parameters	Numerical values
Density of air at 60 m, ρ (kg/m^3)	1.21796
Density of helium inside balloon, ρ_h (kg/m^3)	0.17850
Drag coefficient, c_d	0.47
Radius of helium balloon, R (m)	1.5
Mass of balloon, m_b (kg)	0.056
Length of pulling cord, L (m)	58.5
Length of rotating arm, x_a (m)	0.22
Ground friction coefficient, α	1/7
Sampling time, Δt (s)	1
Sea level standard atmospheric pressure, P_0 (kPa)	101.325
Sea level standard temperature, T_0 (K)	288.15
Temperature lapse rate, Γ (K/m)	0.0065
Earth-surface gravitational acceleration, g (m/s^2)	9.80665
Universal gas constant, R_g ($J/(mol.K)$)	8.31447
Molar mass of dry air, M (kg/mol)	0.028964

Table 5.1 Numerical values of parameters used in simulation

Figure 5.1 displayed the movement of helium balloons when wind started to collide at different constant speeds that include speeds of 2 m/s, 4 m/s, 6 m/s, and 8 m/s at a height of 60 meters (In the processing of the results of the numerical models, this also included numerical models where wind speeds changed following the wind profile power law). They were displayed as coordinates of helium balloons on an x and y axis at that time. It can be observed from results of the model that wind blew helium balloons far on the vertical axis and reduce the height. When wind speed was higher, helium balloons were blown further on the vertical axis and reduce the height even further.

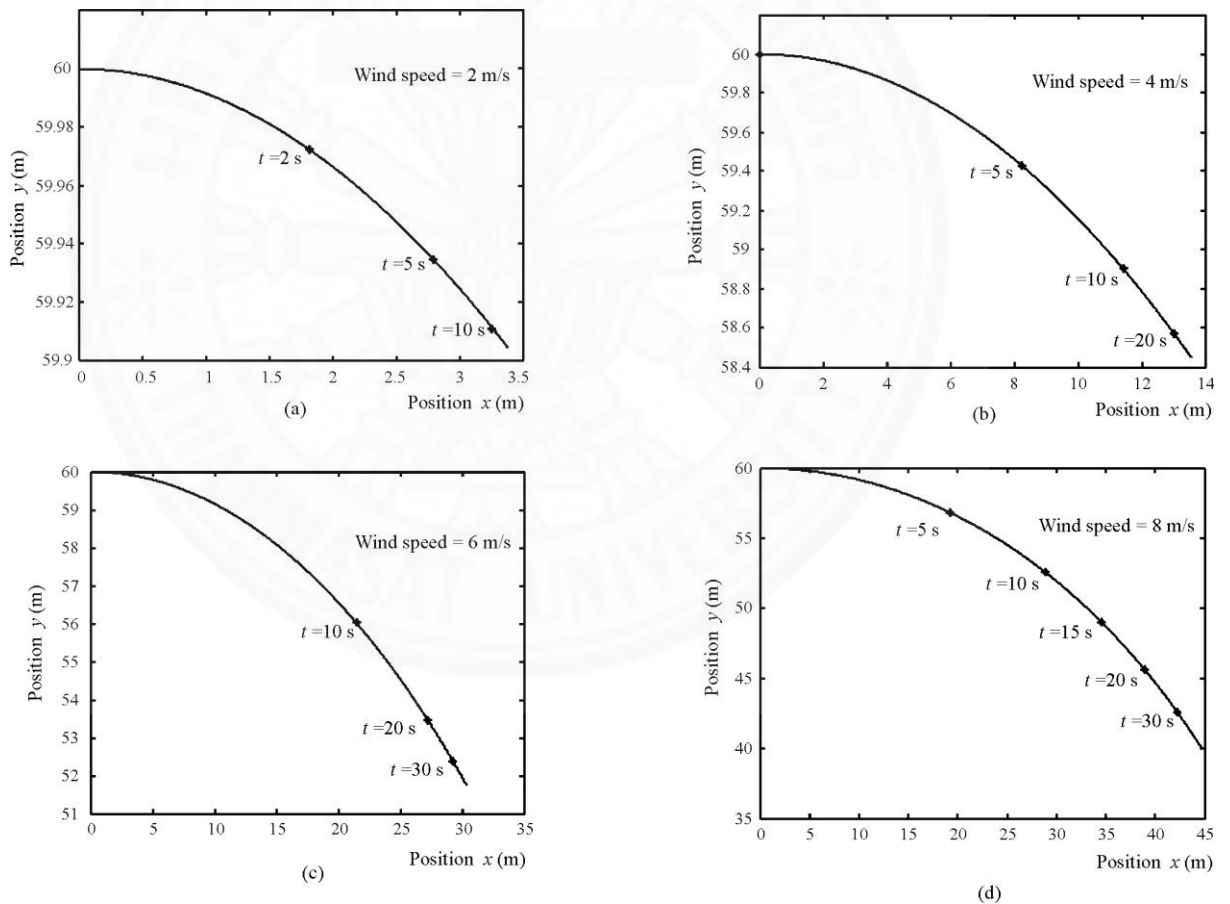


Figure 5.1 Motions of helium balloon at constant wind speed: (a) 2 m/s, (b) 4 m/s, (c) 6 m/s, and (d) 8 m/s

However in the actual situation, natural winds will always have different wind speeds. Figure 5.2 (a) shows the data records of wind speed at a height of 60 meters in one day which were recorded every minute at a 120 meter high wind-mast at Thammasat University. Figures 5.2 (b) and 5.2 (c) displayed the numerical solutions obtained from mathematical modeling, both the coordinates of the helium balloons height and the swing angles between the vertical axis and rope in response to the changes in wind speed that were shown in Figure 5.2 (a) respectively. It can be observed that the movements of helium balloons were propelled by resistance that balanced dynamics and rope tension, buoyancy, and the weight of the helium balloon as explained in chapter 3. Figure 5.3 displayed the graph of wind speed solutions with the use of equations (3.15) and (3.16) in the dotted lines and true wind data from the solid lines. This can be observed from the calculations of wind speed with close values to the actual wind speed, despite changes in the height of the helium balloon.

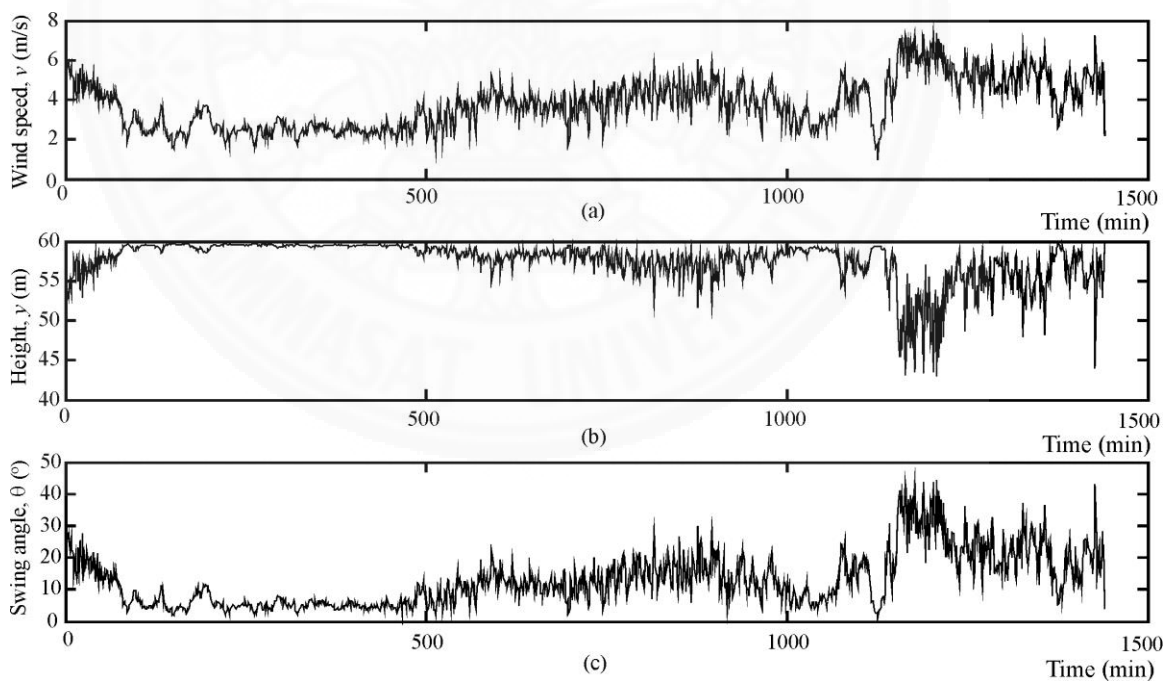


Figure 5.2 Simulated results under real wind blow: (a) actual wind speed, (b) height of helium balloon, and (c) swing angle

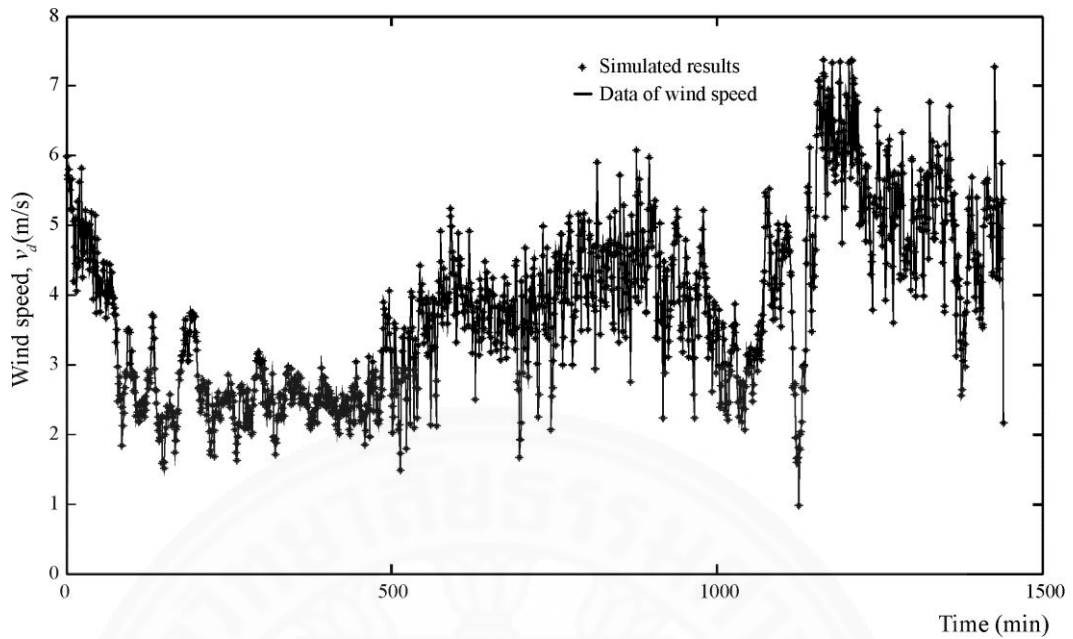


Figure 5.3 Plots of simulated results and measured data of wind speed against time at height of 60 m

This part was an actual experiment in the field as was described in chapter 4, which was to prepare for the experiment with the installation of the rotating arm mechanism close to the wind-mast at a distance of 120 meters away. The data variables that were measured were the angular position of the rotating arm around the vertical axis, the swing angle between the vertical axis and the rope, and rope tension which were received from the movement of the helium balloon in one day. Only the parameter values used in the experiment were different from the numerical models as specified in Table 5.2. Table 5.3 displayed examples of measurement data and solutions from calculations with equations (3.15) and (3.16). The example of calculation are discussed in the Appendix B.

Parameters	Numerical values*
Density of air at 40 m, ρ (kg/m^3)	1.22030
Density of helium inside balloon, ρ_h (kg/m^3)	0.6488
Mass of balloon, m_b (kg)	2.354
Length of pulling cord, L (m)	38.5
Ground friction coefficient, α	0.245

*Remark: The actual values are different than Table 5.1.

Table 5.2 Numerical values of parameters used in experiment

t (s)	θ_y (°)	θ (°)	F_t (N)	v (m/s)	v_d (m/s)	Direction* (°)
1	182.88	26.89	63.43	3.65	3.75	182.88
2	177.84	28.15	63.29	4.36	4.49	177.84
3	178.20	26.78	62.88	3.44	3.53	178.20
4	178.92	27.43	62.23	3.72	3.82	178.92
5	178.56	28.54	63.45	4.45	4.59	178.56
6	178.92	26.82	62.13	3.24	3.33	178.92
7	180.36	26.71	62.98	3.32	3.41	180.36
8	181.08	28.08	63.09	4.35	4.48	181.08
9	180.72	28.29	62.93	4.21	4.34	180.72
10	181.80	28.76	62.10	4.07	4.20	181.80

*Remark: the angle is measured clockwise from a north base line.

Table 5.3 Examples of measured data and determined results

Figure 5.4 displayed the value of ground friction coefficient α , which was 0.245. The value of ground friction coefficient α was determined by using two sets of the measurement device to measure the speed of wind at two different height. In this case, the data of wind speed were measured at height 20 meter and 35 meter as shown in Figure 5.5.

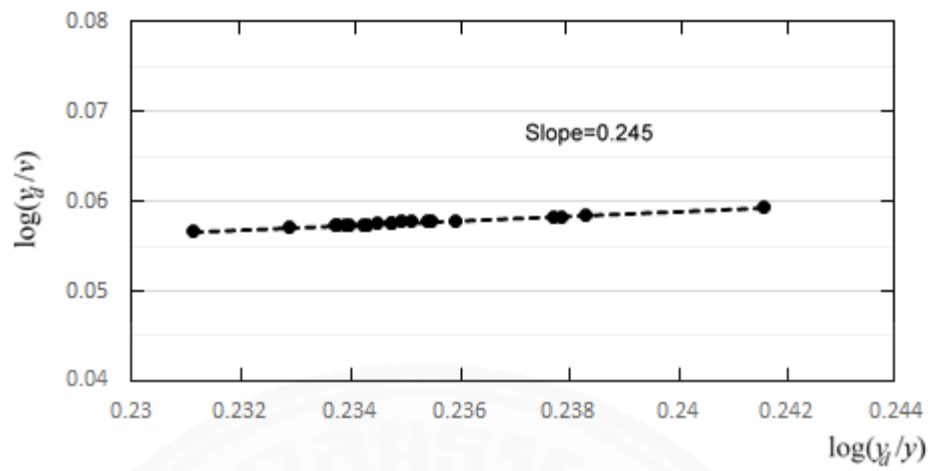


Figure 5.4 Determination of ground friction coefficient α



Figure 5.5 Determination of ground friction coefficient by using two sets of measurement device.

Figure 5.6 displayed the comparisons between wind speed data that were measured from the wind mast and wind speed values from the methods explained in chapter 4. It can be seen that the calculated values had close values with the actual measured wind speed and direction. The error values for the wind speed and direction were equal to 4.136% and $2.79^\circ \pm 0.681^\circ$ respectively. Even so concerning this method of helium balloon anemometer wind measurement, in the case of higher mean wind speeds, adjustment of the balloon's components for more buoyancy is necessary for the preservation of floatation in the vertical axis or to make the helium balloon float at levels where speed measurements are most required. Examples include increases in balloon size or helium gas pressure to prevent the swing angle between the vertical axis and rope from being too large, which will result in minimal inaccuracies with the assessment of wind speed according to the wind profile power law.

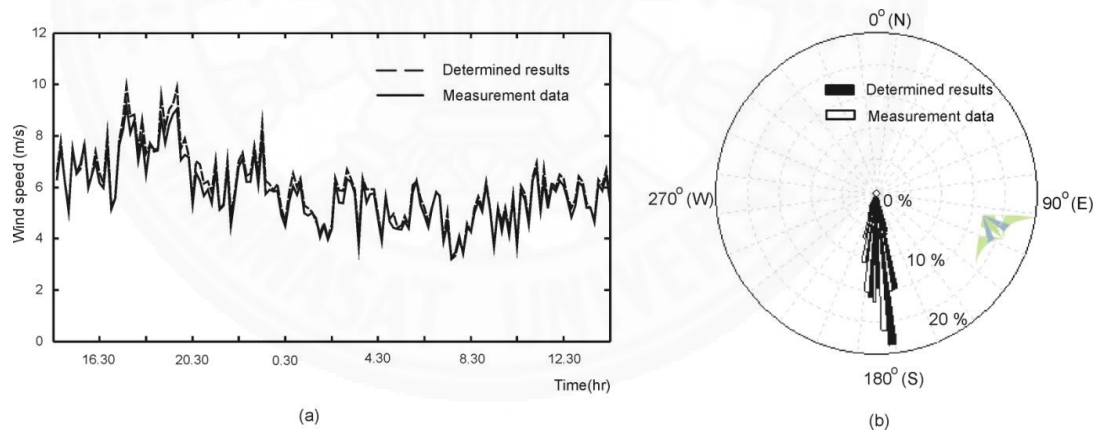


Figure 5.6 Plots of experimental results reported in one day: (a) wind speed against time and (b) wind rose diagram of wind direction

In this studies, the balloon was assumed to be a particle floating in the large atmosphere. The wind usually flows through the balloon in horizontal direction. However, in some cases, due to various factor such as weather or environment condition, the vertical wind might occur. The algorithm to compute the vertical wind speed is the same as the horizontal wind speed's which is determining the vertical acceleration and vertical velocity of balloon. Figure 5.7 displayed the wind speed data in vertical direction or in y-axis that was measured from the measurement device. It can be seen that the wind speeds in y-axis are less than 1 m/s. The wind speeds in vertical direction with very low value have very low influence on the wind speed in horizontal direction.

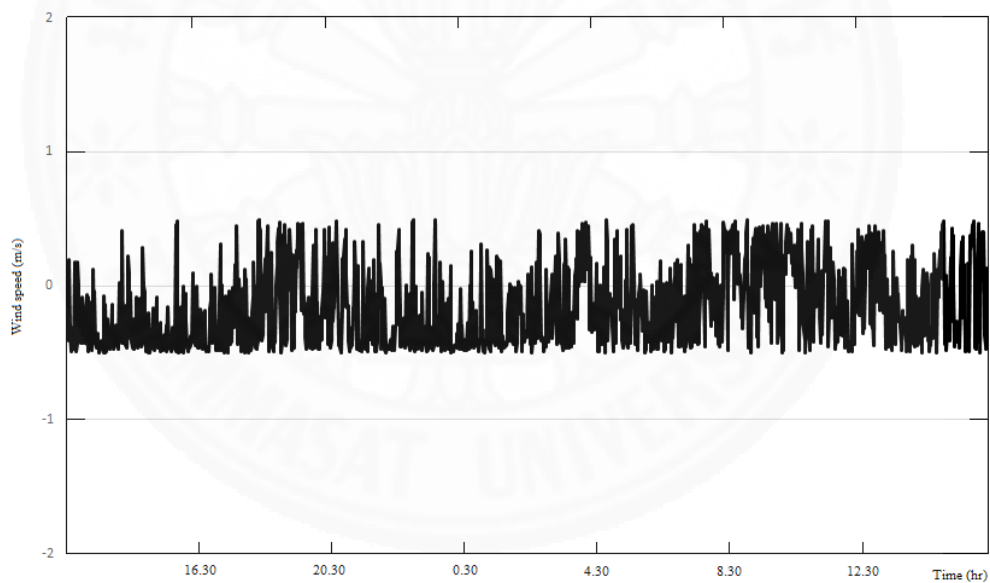


Figure 5.7 Plots of experimental results of wind speed in y-axis against time

Chapter 6

Conclusions

6.1 Conclusions

The main objective of the study was the presentation of an alternative method of wind measurement via interpreting dynamic behaviors of a helium balloon where wind speed was calculated from some variables in the mathematical models based on the aerodynamic behavior within the movement of helium balloons. In this study, balloons with a diameter of 3 meters and filled with helium gas were used while the measurement device comprised of a helium balloon held by rope to a rotating arm mechanism that rotates according to wind direction. Its principles detail that when wind blows, the resistance formed from wind will balance the dynamics of buoyancy, the weight of the helium balloon, and rope tension. Thus the wind speed at the balloon's height can be determined from equations of movement, resistance, and variables obtained from the balloon's measurements include the coordinates of the helium balloon's height, the swing angles between the vertical axis and rope, and rope tension and the application of the wind profile power law. The wind speed at the balloon's height can be adjusted to be the speed value at the height of measurement interest by apply the wind profile power law. Results from experiments in the field discovered that wind speed values obtained from the measurement device and values wind-mast were highly similar, which displayed the good potential of the proposed helium balloon anemometer of the efficiency of the helium balloon method of wind measurement, in the case that the wind speeds are higher than this, adjustments for helium balloons is necessary to have more buoyancy to preserve floatation in the vertical axis or to make the helium balloon float at levels where speed measurements are most required such as increases in balloon size or helium gas pressure to prevent the swing angle between the vertical axis and rope from being too large will result in minimal inaccuracies with the assessment of wind speed according to the wind profile power law.

However, the helium gas contained in the balloon usually leaks out. Therefore, it requires frequent maintenance to fill up the helium gas. In the future, new technology of balloon might be developed to be able to sustain helium gas inside. Then, this device can be used practically.

6.2 Future work

According to the result of measuring wind speed and wind direction, it confirms that there is very good agreement of wind measurement on the measurement device compared to the conventional anemometer and the wind vane mounted on the wind mast. However, there is still leakage of the helium gas in the balloon during the measurement causing some errors on the measurement result. It is possible that the measurement device can be improved to be more compact and more precise in wind measurement. This could be performed by utilizing newer technology as well as modern equipment to develop the measurement device.

References

Books and Book Articles

Bañuelos-Ruedas, F., Angeles-Camacho, A., and Rios-Marcuello, S. (2011). *Methodologies Used in the Extrapolation of Wind Speed Data at Different Heights and Its Impact in the Wind Energy Resource Assessment in a Region*, Intech.

Barthelmie, R., Hansen, O.F., Enevoldsen, K., Højstrup, J., Frandsen, S., Pryor, S., Larsen, S., Motta, M., and Sanderhoff, P. (2005). Ten years of meteorological measurements for offshore wind farms, *Journal of Solar Energy Engineering*, 127(2), 170-176.

Bertin, J.J., and Smith, M.L., (1998). *Aerodynamics for engineers*, Prentice Hall.

Brown, W.O.J., Cohn, S.A., Susedik, M.E., Martin, C.L., Maclean, G., and Parsons, D.B. (1999). The NCAR/ARM multiple antenna profiler, *Proceeding of 9th ARM Science Team Meeting, San Antonio, Texas, 22-26 March 1999* (pp. 1-7)

Chen, K., Song, M.X., and Zhang, X. (2013). A statistical method to merge wind cases for wind power assessment of wind farm, *Journal of Wind Engineering and Industrial Aerodynamics*, 119, 69-77.

Emeis, S. (2010). *Measurement methods in atmospheric sciences: in situ and remote*, Schweizerbart Science.

Klink, K. (2007). Atmospheric circulation effects on wind speed variability at turbine height, *Journal of Applied Meteorology Climatology*, 46(4), 445–456.

Lataitis, R.J., Clifford, S.F., and Holloway, C.L. (2005). An Alternative Method for Inferring Wind from Spaced-antenna Radar Measurements, *Radio Science*, 30(2), 463-474.

Leephakpreeda, T. (2010). Application of DC Servomotor on Airflow Measurement, *Journal of Dynamic Systems, Measurement and Control*, 132(2), 1-7

Mukund R. Patel. (1999). *Wind and solar power systems*, New York, CRC Press.

Oh, K.Y., Kim, J.Y., Lee, J.K., Ryu, M.S., and Lee, J.S. (2012). An assessment of wind energy potential at the demonstration offshore wind farm in Korea, *Energy*, 46(1), 555-563.

Shen, F., Cha, H., Sun, D., Kim, D., and Ok kwon, S. (2008). Low Tropospheric Wind Measurement with Mie Doppler Lidar, *OPTICAL REVIEW*, 15(4), 204–209.

Song, M.X., Chen, K., He, Z.Y., and Zhang, X. (2014). Wind resource assessment on complex terrain based on observations of a single anemometer, *Journal of Wind Engineering and Industrial Aerodynamics*, 125, 22-29.

Treddenick, D.S., National Aeronautics Establishment, National Research Council of Canada, Ottawa. (1971). A comparison of Aircraft and Jimsphere Wind Measurements, *Journal of applied methodology*, 10, 309–312.

Wu, D., Tang, J., Liu, Z., and Hu, Y. (2012). Simulation of coherent Doppler wind lidar measurement from space based on CALIPSO lidar global aerosol observations, *Journal of Quantitative Spectroscopy and Radiative Transfer*, 122, 79-86.

Electronic Media

Bellis, M. (n.d.). *History of the Anemometer*. Retrieved from January 18, 2015, <http://inventors.about.com/od/astartinventions/a/Anemometer.htm>

Cohn, S.A., Brown, W.O.J., Martin, C.L., Susedik, M.E., Maclean, G.D., and Parsons, D.B. (2001). Clear air boundary layer spaced antenna wind measurement with the Multiple Antenna Profiler (MAPR) [Electronic version]. *Annales Geophysicae*, 19, 845–854

Pratt, C.S. (2008). *Wind Vanes and Weather Vanes*. Retrieved from January 10, 2015, http://www.growingseasons.com/Growing_Seasons/Wind_Vanes___Weather_Vanes.html



Appendices

Appendix A

Dimension* of mechanism device

Equipment & Material

1. 2 Rotary potentiometer: used for measuring the angle of swing arm and the angle between rope and vertical line of helium balloon.
2. 1 Linear potentiometer: used for measuring the tension of cord.
3. 3 Ball bearing: used for rotation of swing arm and rotate the mechanism device of velocity part.
4. 1 Spring: used with the linear potentiometer to measure the tension of cord.
5. 1 Balloon of 3 meters diameter: used to release to the desired height to measure the wind speed and wind direction.
6. Stainless steel: used to make the rotating base.
7. Aluminium: used to make the measurement device of velocity part.

*Remark: All dimension are in millimeter.

Figure A.1 (a) and (b) shows the design of measurement device and each components of the device respectively.

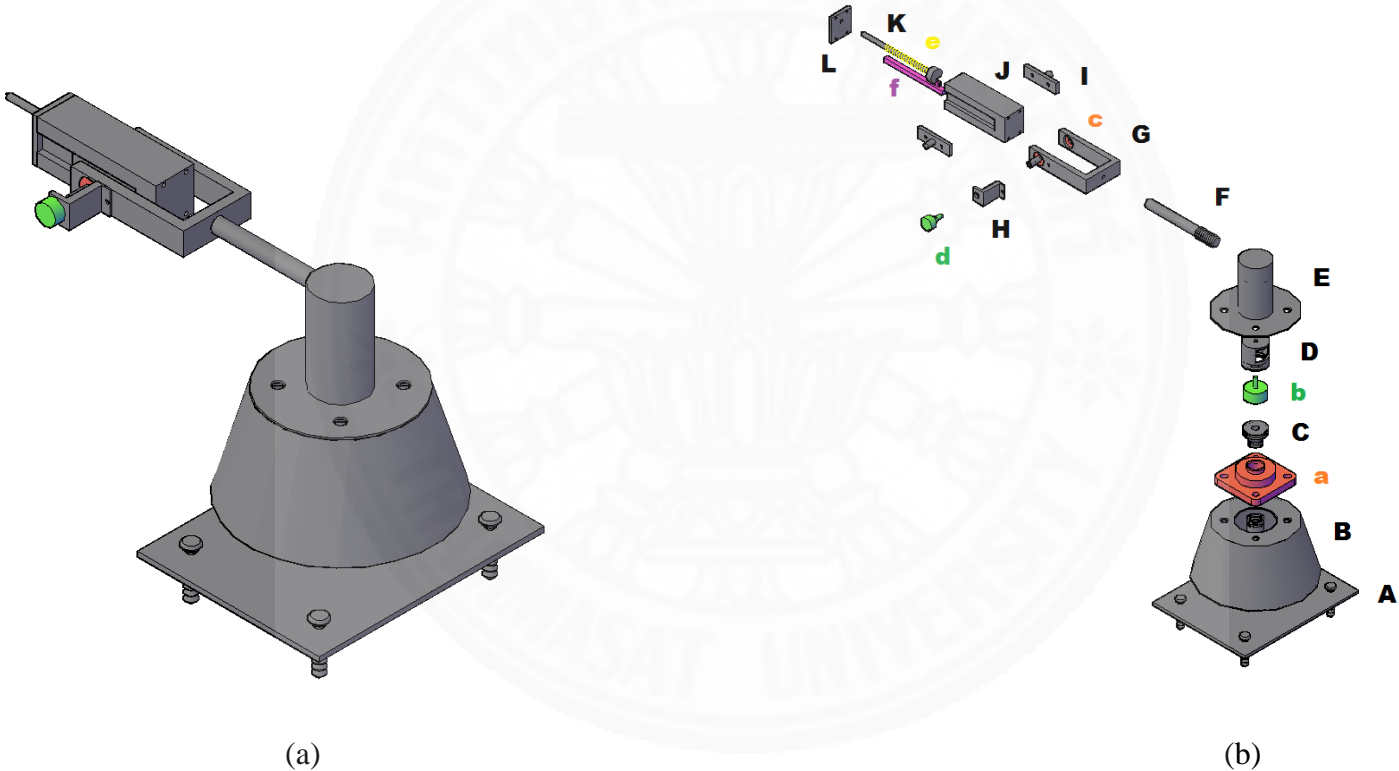


Figure A.1 The measurement device (a) completely assembled (b) Decomposition

Figure A.2 shows the drawing dimension of the component part A in first angle projection.

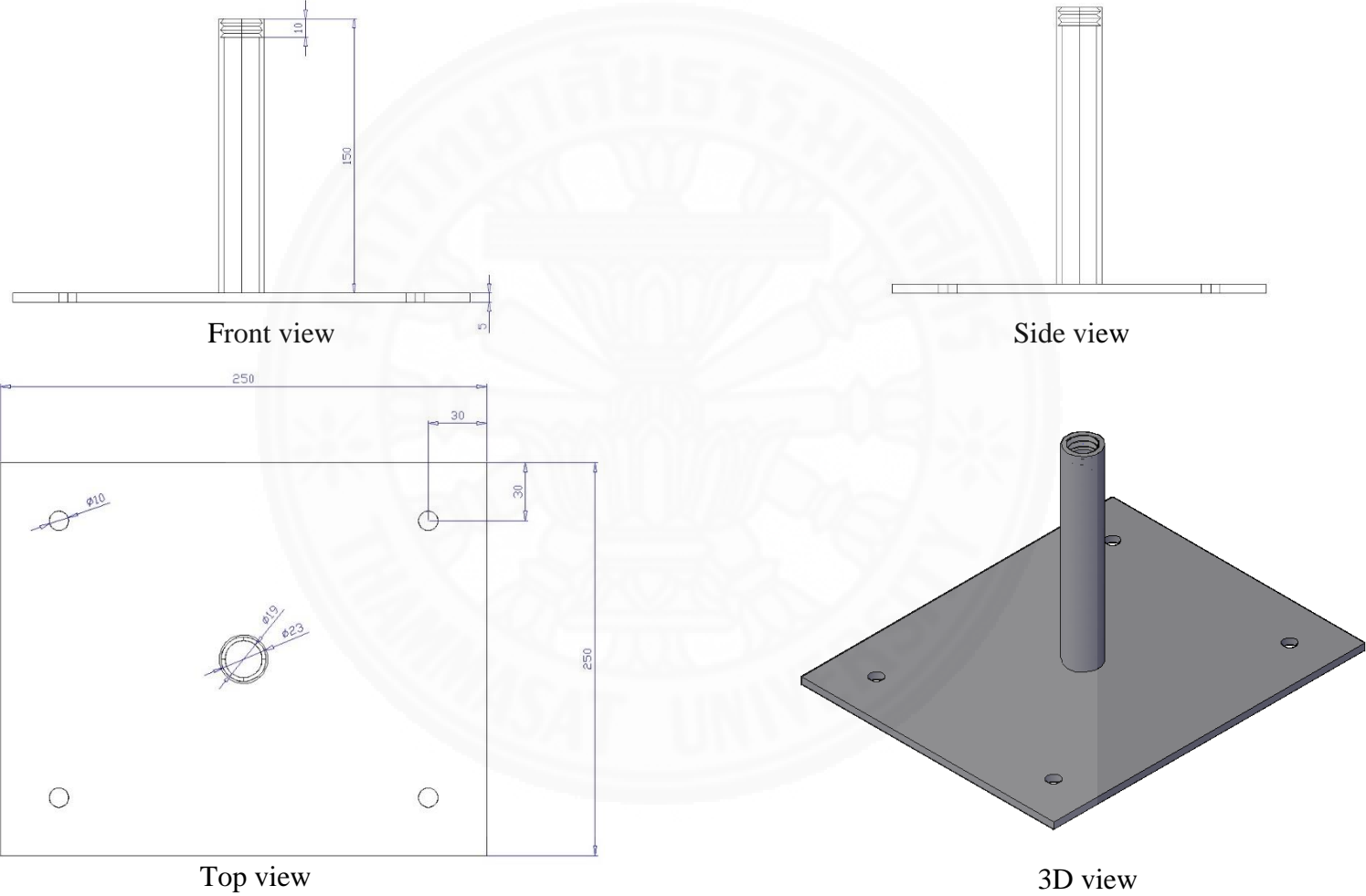


Figure A.2 Orthographic drawing of part A

Figure A.3 shows the drawing dimension of the component part B in first angle projection.

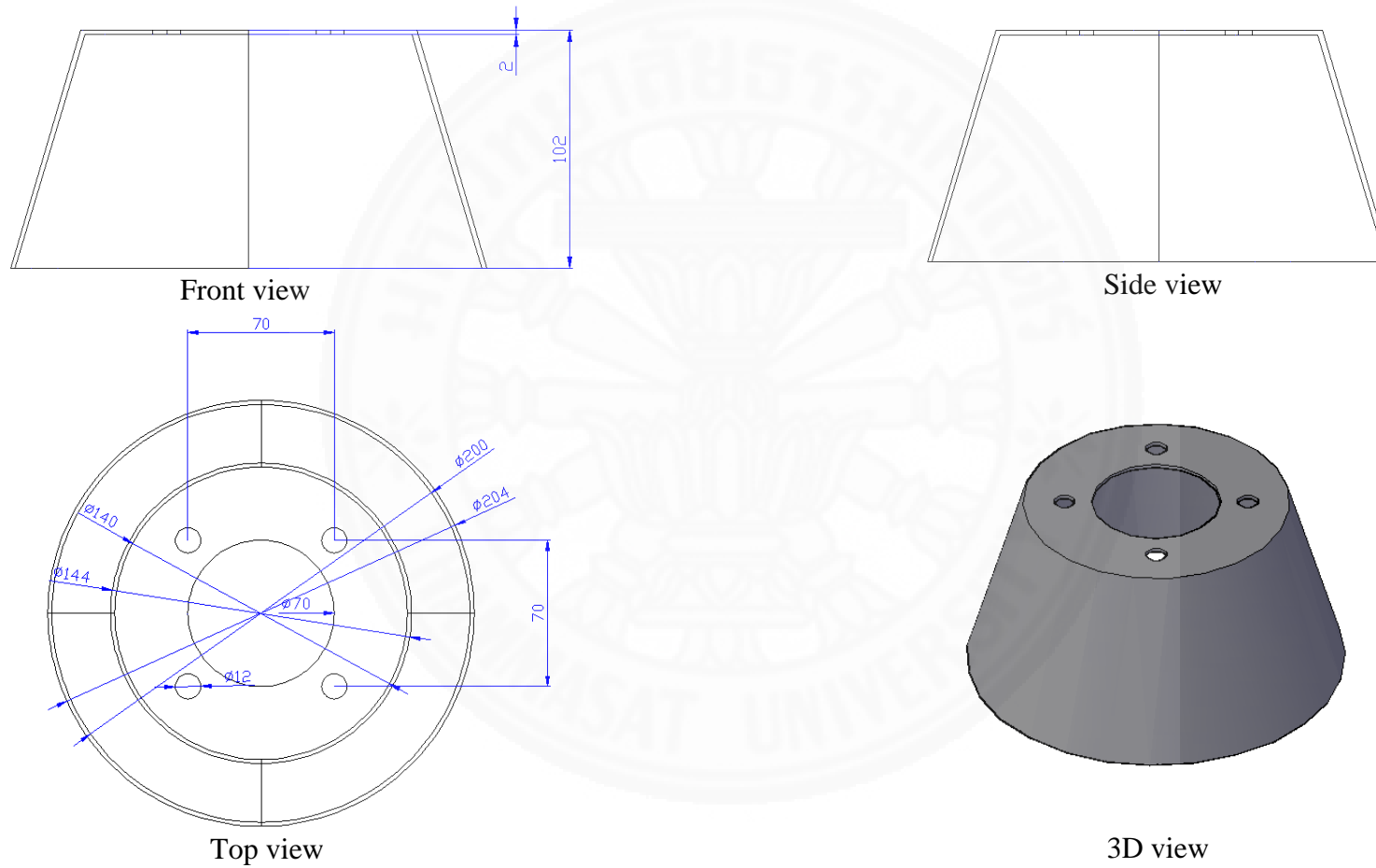


Figure A.3 Orthographic drawing of part B

Figure A.4 shows the drawing dimension of the component part C in first angle projection.

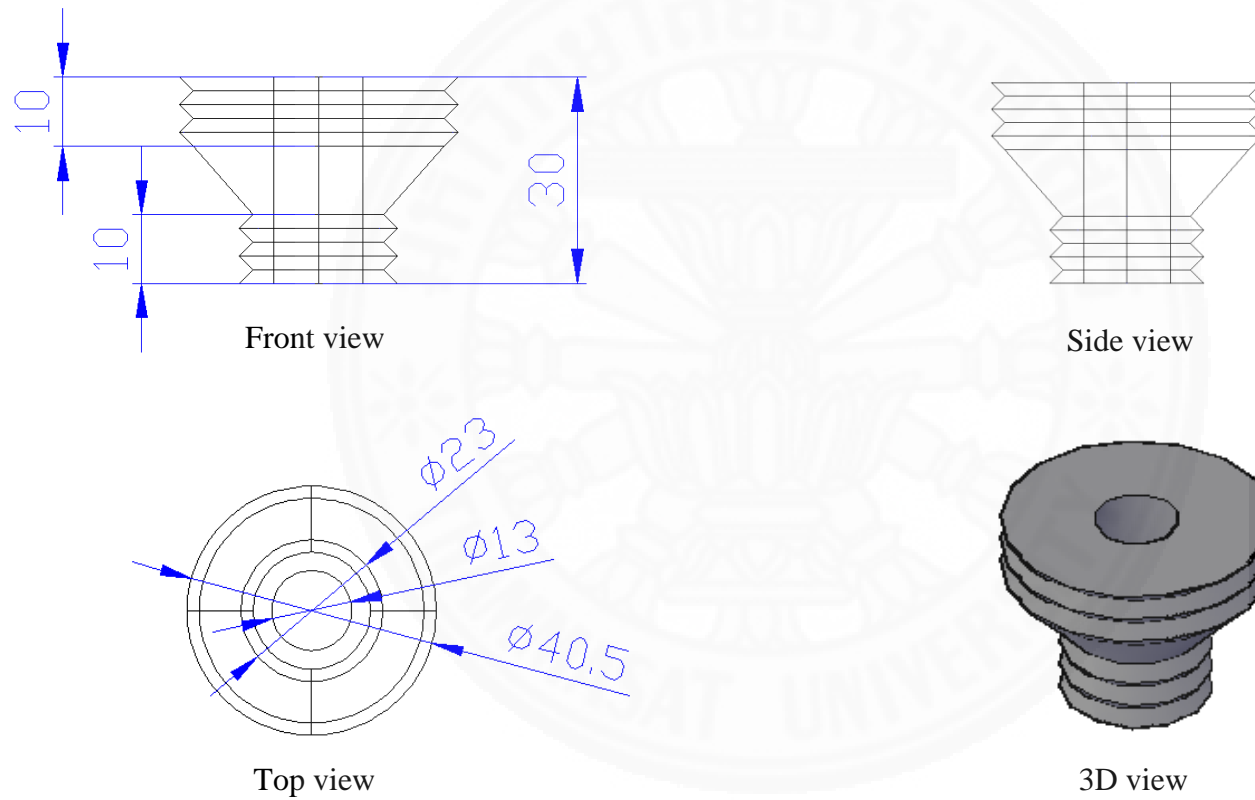


Figure A.4 Orthographic drawing of part C

Figure A.5 shows the drawing dimension of the component part D in first angle projection.

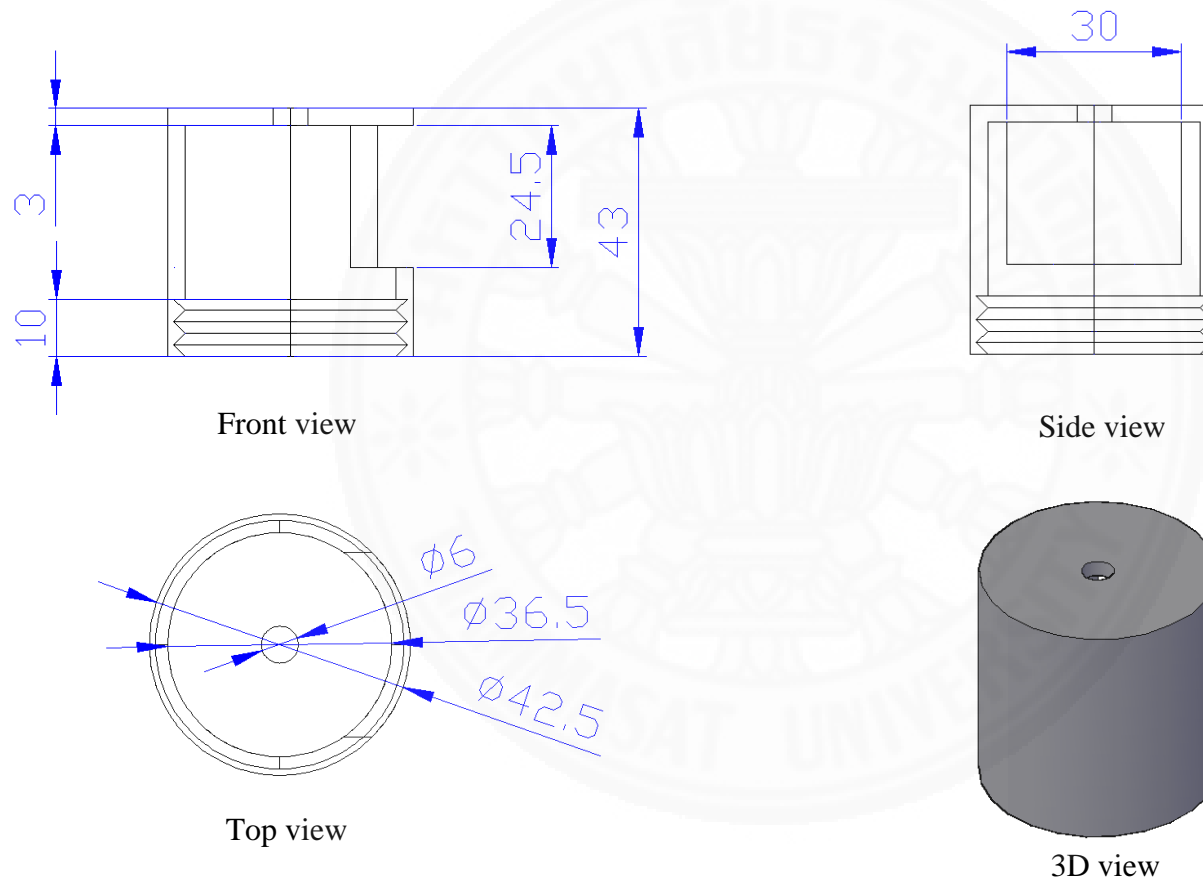


Figure A.5 Orthographic drawing of part D

Figure A.6 shows the drawing dimension of the component part E in first angle projection.

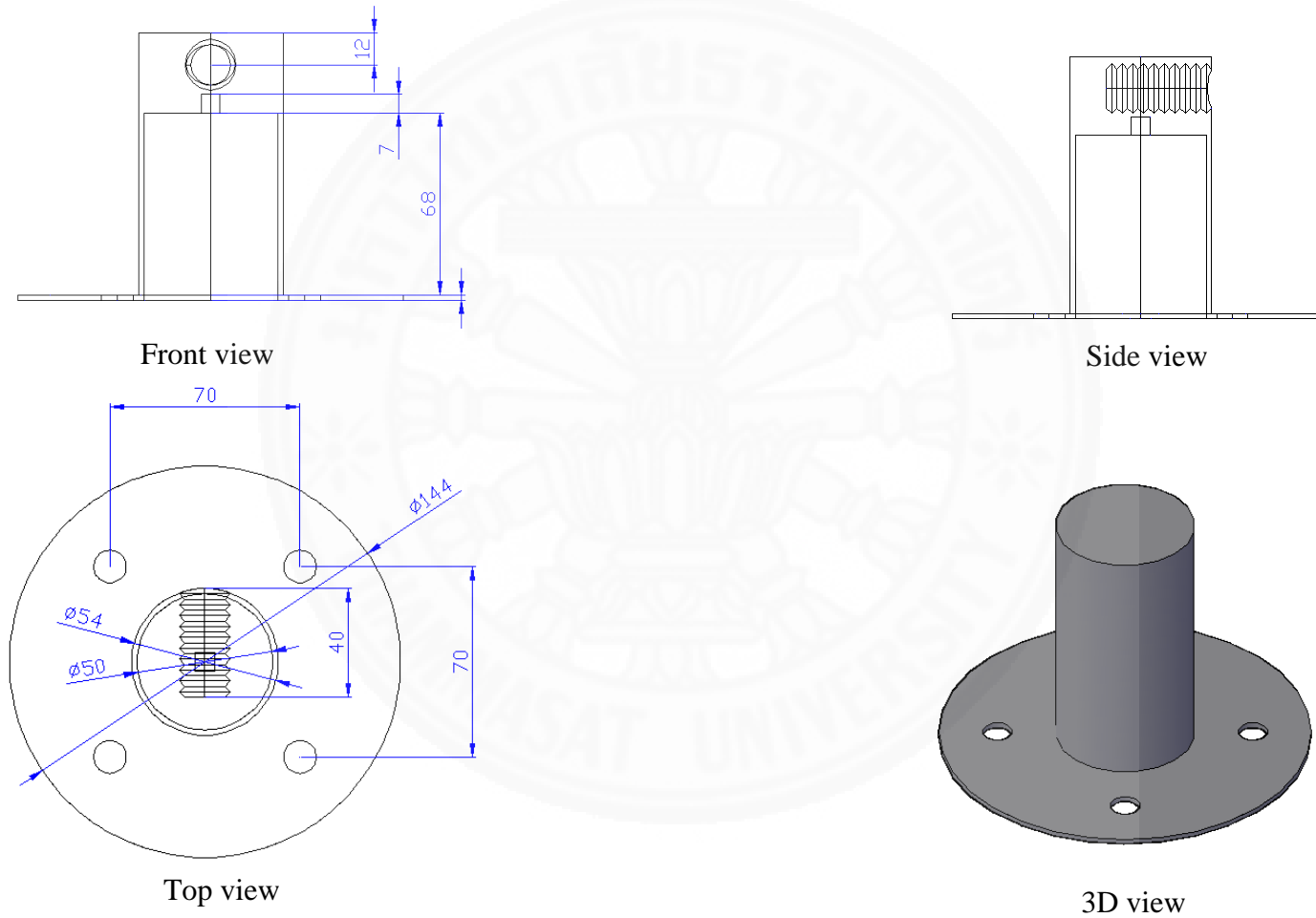


Figure A.6 Orthographic drawing of part E

Figure A.7 shows the drawing dimension of the component part F in first angle projection.

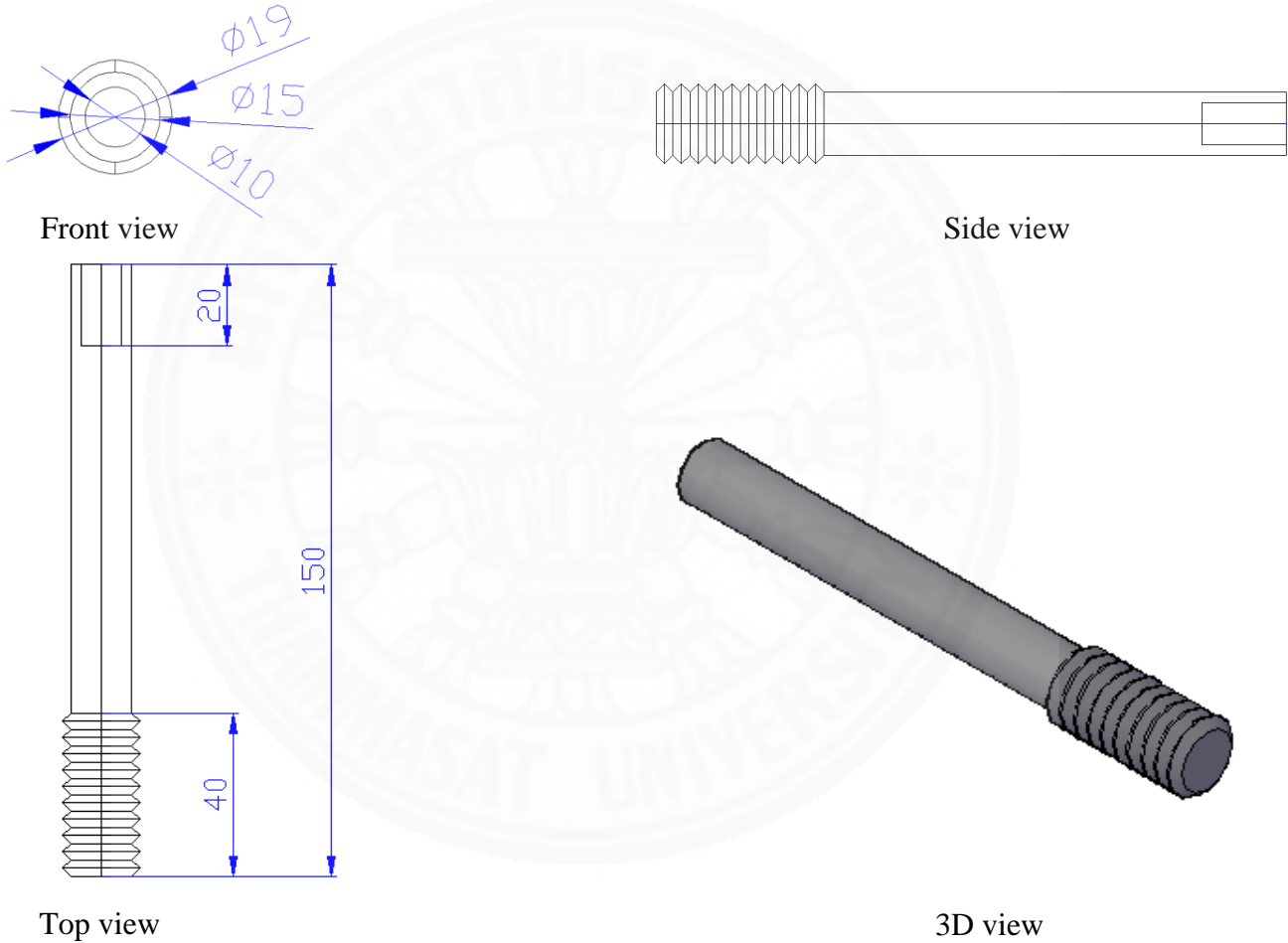


Figure A.7 Orthographic drawing of part F

Figure A.8 shows the drawing dimension of the component part G in first angle projection.

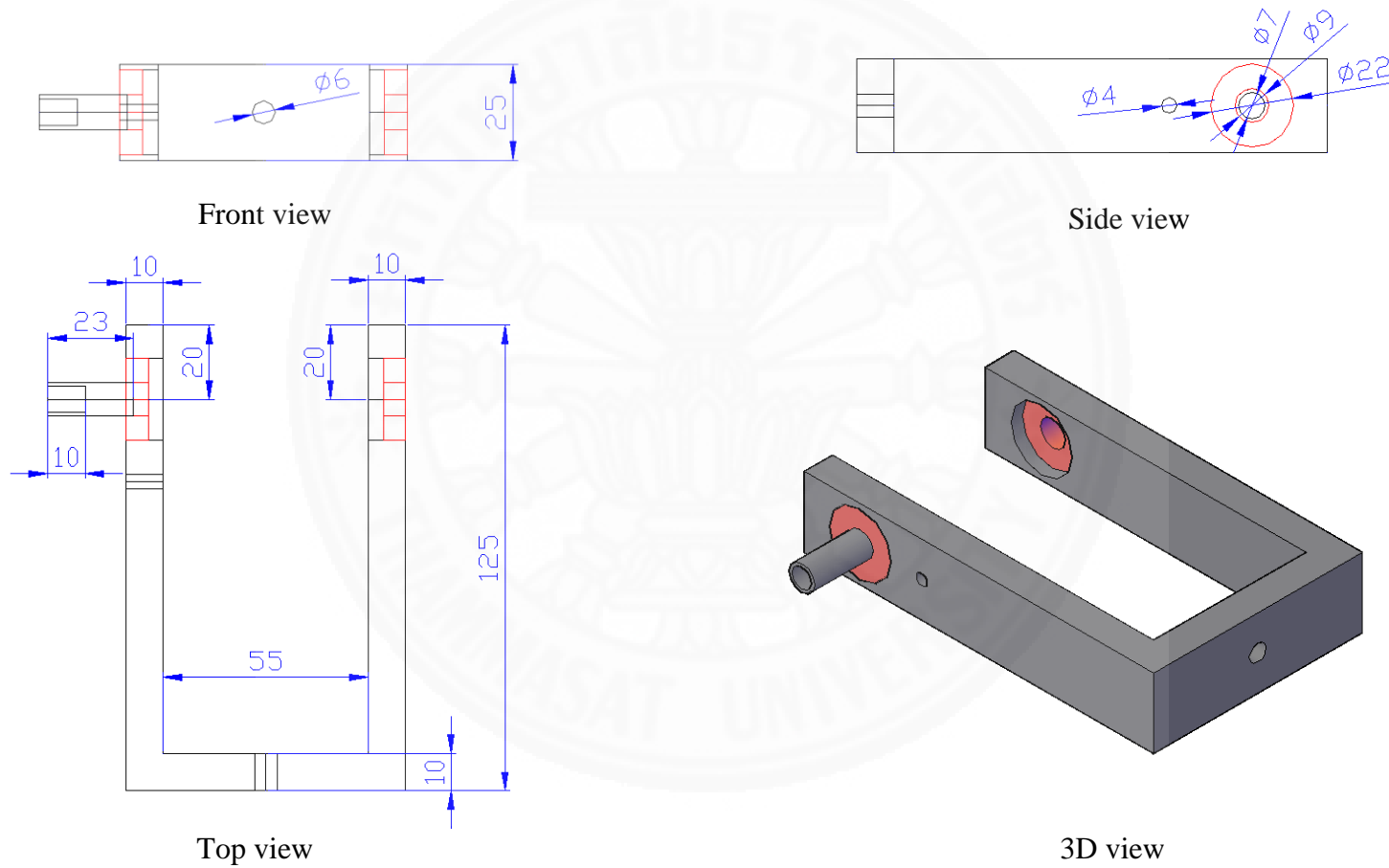


Figure A.8 Orthographic drawing of part G

Figure A.9 shows the drawing dimension of the component part H in first angle projection.

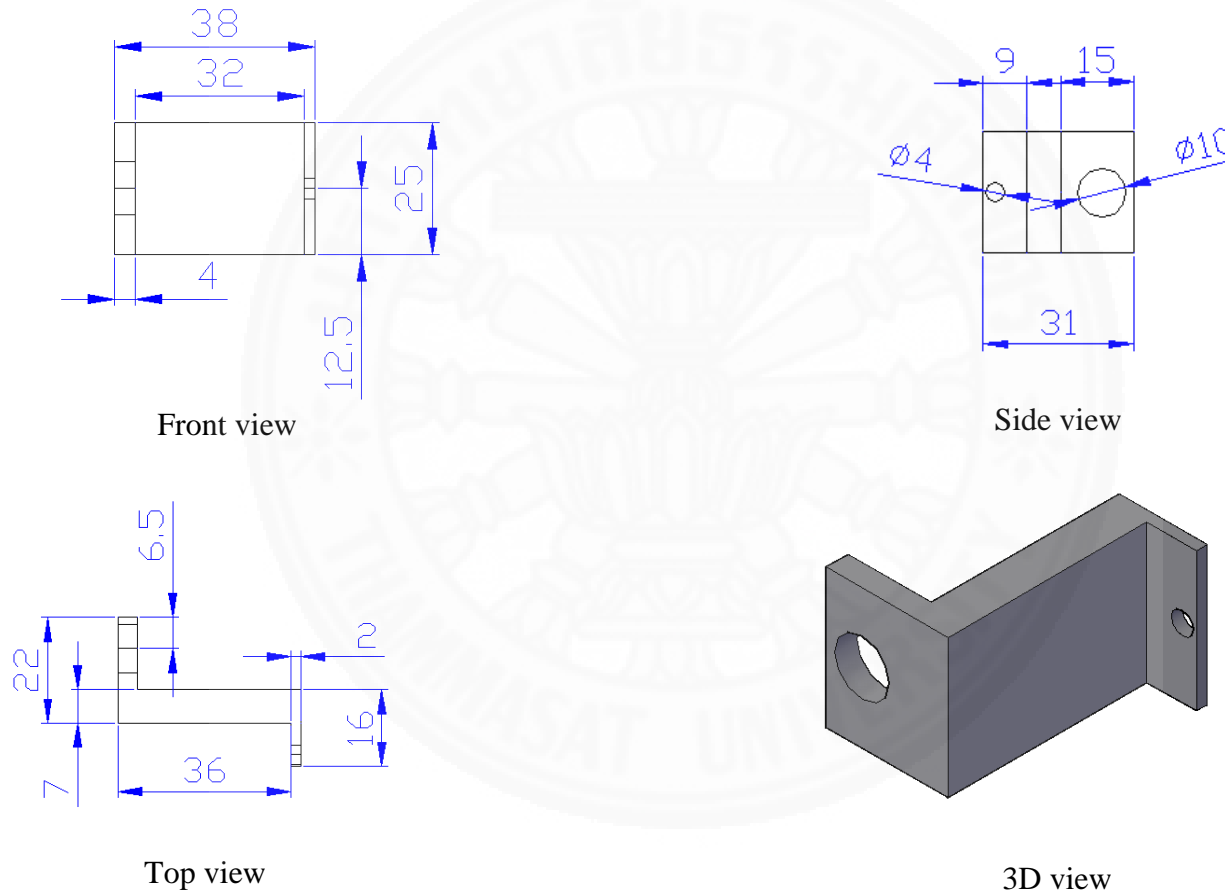


Figure A.9 Orthographic drawing of part H

Figure A.10 shows the drawing dimension of the component part I in first angle projection.

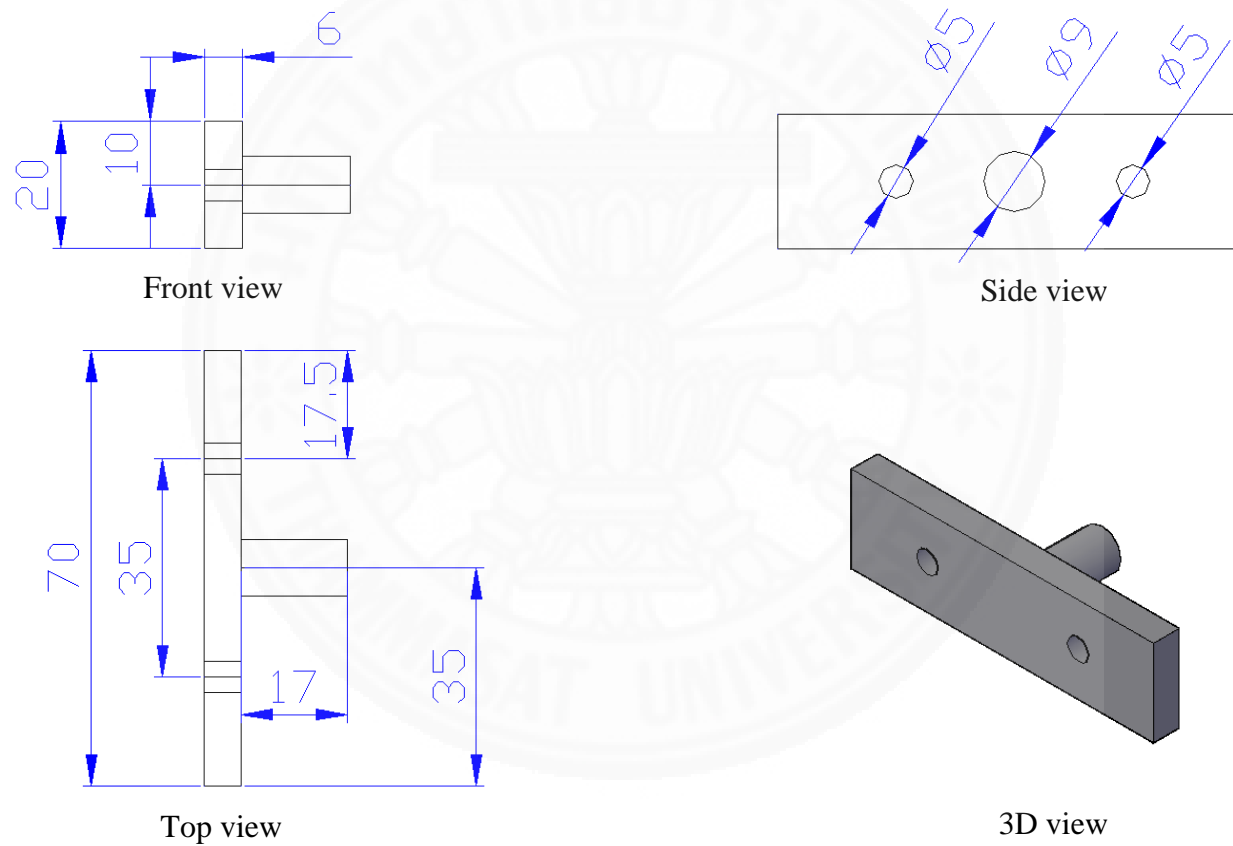


Figure A.10 Orthographic drawing of part I

Figure A.11 shows the drawing dimension of the component part J in first angle projection.

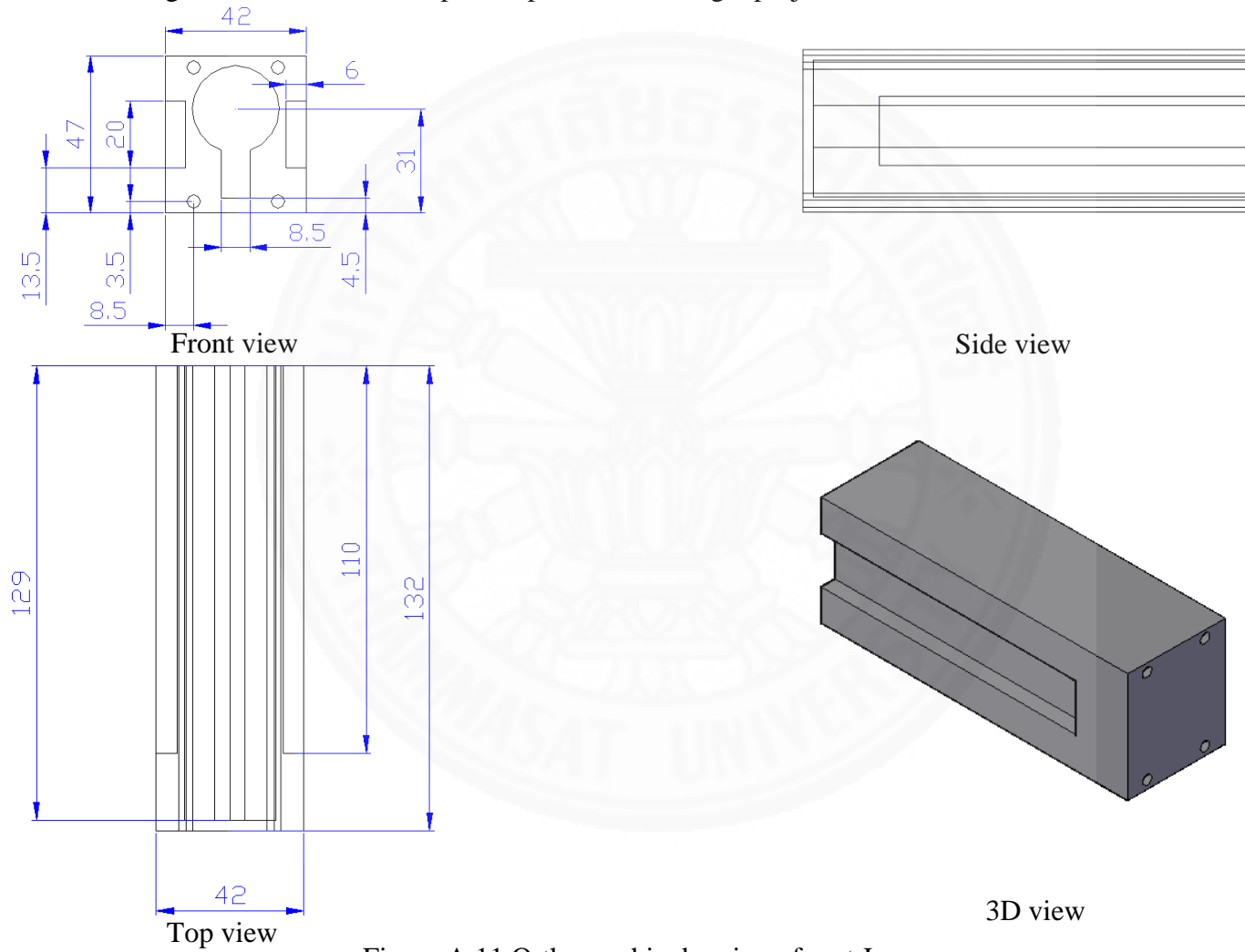


Figure A.11 Orthographic drawing of part J

Figure A.12 shows the drawing dimension of the component part K in first angle projection.

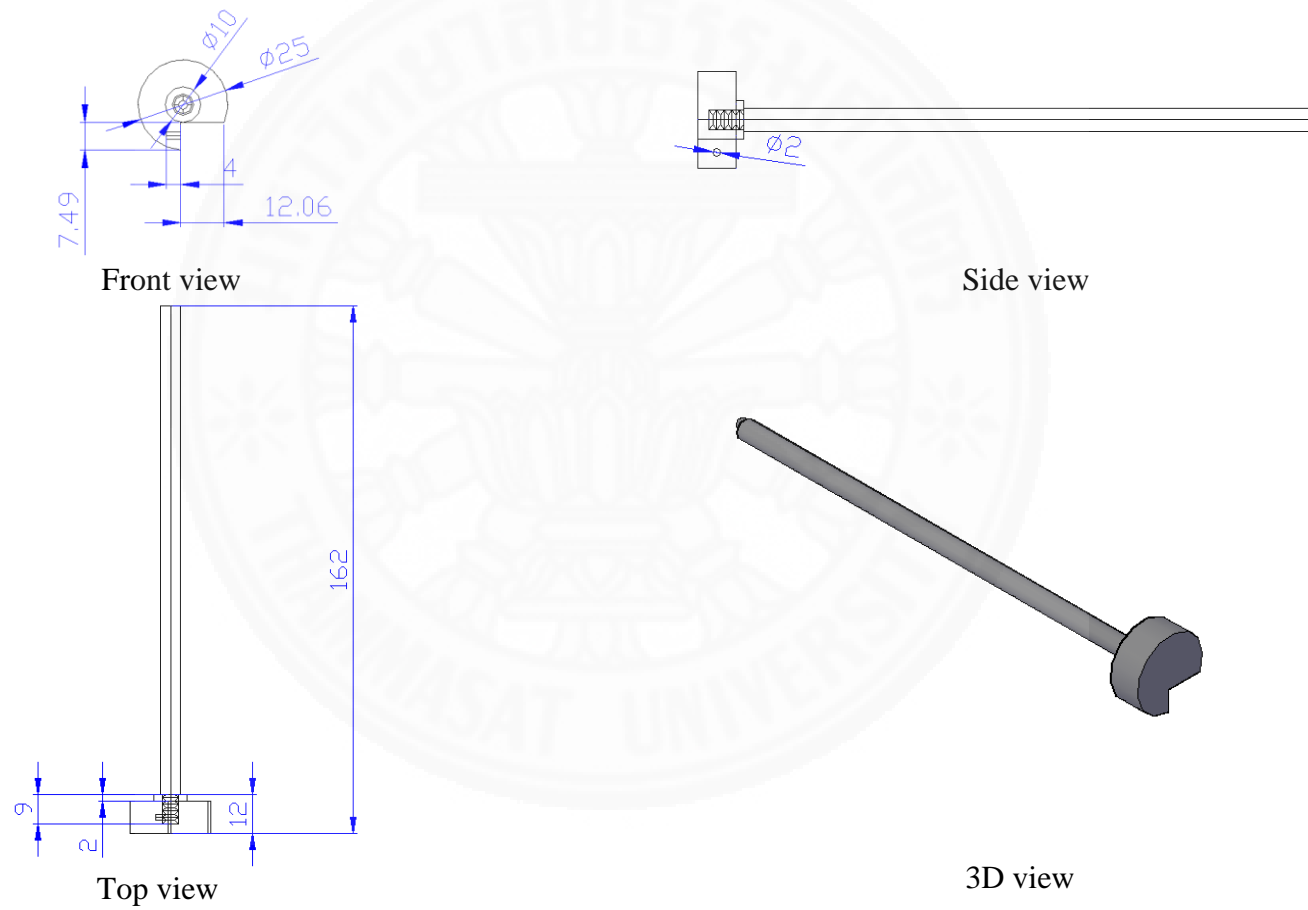


Figure A.12 Orthographic drawing of part K

Figure A.13 shows the drawing dimension of the component part L in first angle projection.

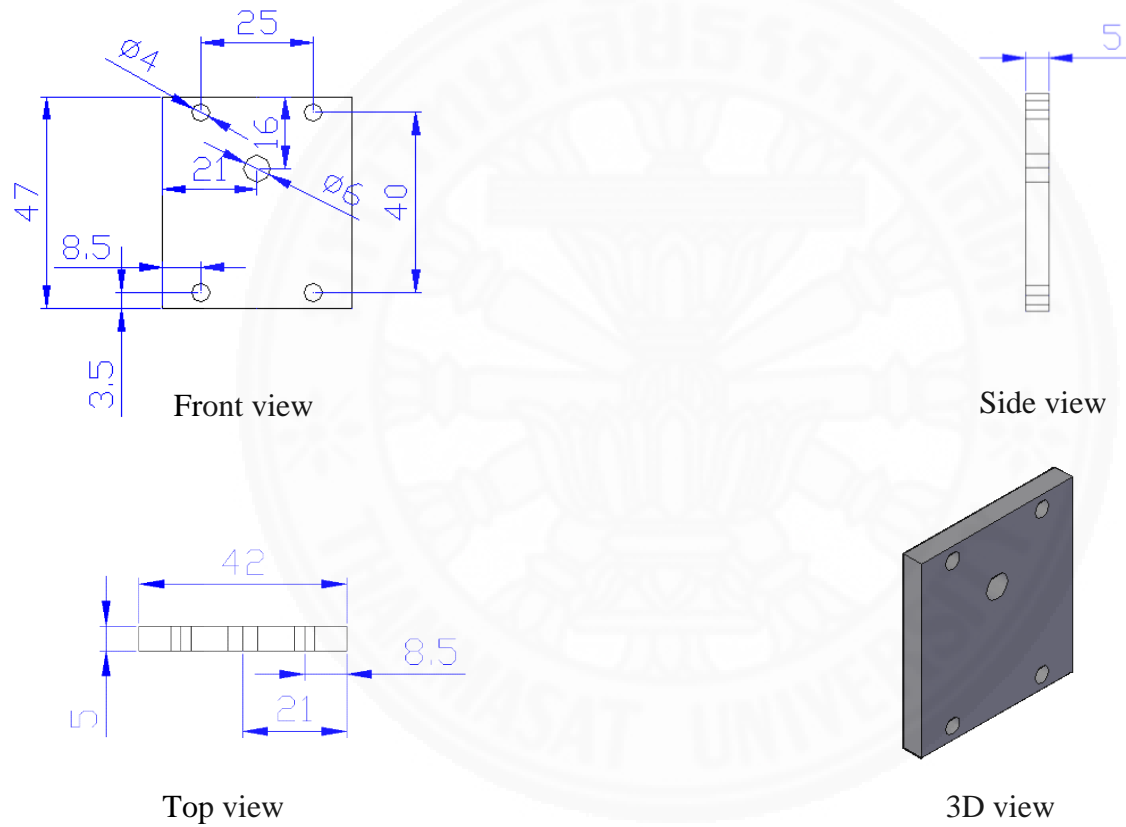


Figure A.13 Orthographic drawing of part L

Appendix B

Example of calculation

Example of the experiment data of wind measurement by using helium balloon anemometer.

	A	B	C	D	E	F	G	H	I	J	K	L	M
1	Date	Time	Tension(K Ω)	Angle(K Ω)	Spring(m)	Tension(N)	Angle ($^{\circ}$)	X(m)	Y(m)	\ddot{x} (m/s 2)	V $_b$ (m/s)	V(m/s)	V power law (m/s)
2	4/1/2014	2:30:00 PM	3.803	0.774	0.03803	61.9889	27.864	18.57813382	35.42390357	-	-	-	-
3	4/1/2014	2:30:01 PM	3.827	0.717	0.03827	62.3801	25.812	17.30793117	36.0615518	-	-	-	-
4	4/1/2014	2:30:02 PM	3.899	0.716	0.03899	63.5537	25.776	17.28544398	36.07233603	1.247715448	-0.646344919	3.237309462	3.320329766
5	4/1/2014	2:30:03 PM	3.865	0.783	0.03865	62.9995	28.188	18.77655545	35.31913031	1.513598663	0.734312137	4.788754175	4.937018917
6	4/1/2014	2:30:04 PM	3.814	0.718	0.03814	62.1682	25.848	17.33041153	36.05075361	-2.937255379	0.022483778	3.178476449	3.260466036
7	4/1/2014	2:30:05 PM	3.804	0.773	0.03804	62.0052	27.828	18.55605018	35.4354766	2.671782556	-0.110252633	4.058931659	4.18123001
8	4/1/2014	2:30:06 PM	3.828	0.71	0.03828	62.3964	25.56	17.15037782	36.13674779	-2.631311009	-0.090016859	3.107676972	3.185980012
9	4/1/2014	2:30:07 PM	3.899	0.763	0.03899	63.5537	27.468	18.33481235	35.55045226	2.5901069	-0.110618914	4.069017175	4.188294042
10	4/1/2014	2:30:08 PM	3.869	0.744	0.03869	63.0647	26.784	17.91247358	35.76511275	-1.60677331	0.381047881	3.867270655	3.974766894
11	4/1/2014	2:30:09 PM	3.892	0.747	0.03892	63.4396	26.892	17.97932991	35.73155043	0.489195107	-0.17774122	3.659412801	3.761996567
12	4/1/2014	2:30:10 PM	3.883	0.782	0.03883	63.2929	28.152	18.75453813	35.33082648	0.708351887	0.421032277	4.364945782	4.499723949
13	4/1/2014	2:30:11 PM	3.858	0.744	0.03858	62.8854	26.784	17.91247358	35.76511275	-1.617272775	-0.033428167	3.445321153	3.54108871
14	4/1/2014	2:30:12 PM	3.818	0.762	0.03818	62.2334	27.432	18.31264861	35.56187426	1.24223959	-0.220944759	3.727035383	3.835985672
15	4/1/2014	2:30:13 PM	3.893	0.793	0.03893	63.4559	28.548	18.99631945	35.20141826	0.283495795	0.541922934	4.452092191	4.593689187
16	4/1/2014	2:30:14 PM	3.812	0.745	0.03812	62.1356	26.82	17.93476611	35.75393915	-1.745224171	-0.188941254	3.246697567	3.337199568
17	4/1/2014	2:30:15 PM	3.864	0.742	0.03864	62.9832	26.712	17.86786732	35.78741843	0.99465455	-0.564226065	3.3244458	3.416331567
18	4/1/2014	2:30:16 PM	3.871	0.78	0.03871	63.0973	28.08	18.7104813	35.35417782	0.909512776	0.387857599	4.351193565	4.484821058
19	4/1/2014	2:30:17 PM	3.861	0.786	0.03861	62.9343	28.296	18.84256287	35.28395987	-0.710532416	0.487347779	4.21454612	4.3460935
20	4/1/2014	2:30:18 PM	3.81	0.799	0.0381	62.103	28.764	19.12781843	35.13013752	0.153173983	0.208668562	4.071372014	4.202947079
21	4/1/2014	2:30:19 PM	3.845	0.8	0.03845	62.6735	28.8	19.14970855	35.11820984	-0.263365436	0.153572836	3.973155717	4.101897971
22	4/1/2014	2:30:20 PM	3.834	0.771	0.03834	62.4942	27.756	18.51186094	35.45858154	-0.659737723	-0.307978744	3.378698138	3.47994482

Example of the experiment data of wind measurement by using helium balloon anemometer.

	A	B	C	D	P	Q	R	S	T	U	V	W	X	Y	Z
1	Date	Time	Tension(KΩ)	Angle(KΩ)	Direction (KΩ)	Dirction (°)		$\ddot{Y}(m/s^2)$	$V_{by}(m/s)$	SIGN \ddot{Y}	$F_{dy}(N)$	$F_{dy} \times \text{SIGN } \ddot{Y}$	$/(p)(A)(C_d)$	$V_y(m/s)$	V power law (m/s)
2	4/1/2014	2:30:00 PM	3.803	0.774	5.065	182.34									
3	4/1/2014	2:30:01 PM	3.827	0.717	5.147	185.292									
4	4/1/2014	2:30:02 PM	3.899	0.716	5.532	199.152		-0.626864013	0.324216	-1	0.641488	-0.641488412	-0.450562868	-0.12635	-0.129586778
5	4/1/2014	2:30:03 PM	3.865	0.783	5.465	196.74		-0.763989945	-0.37121	-1	1.560949	-1.560948945	-1.096365298	0.725155	0.747606078
6	4/1/2014	2:30:04 PM	3.814	0.718	5.321	191.556		1.484829028	-0.01079	1	1.810458	1.810457862	1.27161313	1.260822	1.293345136
7	4/1/2014	2:30:05 PM	3.804	0.773	5.252	189.072		-1.346900321	0.058173	-1	2.12183	-2.121829827	-1.490311773	-1.43214	-1.475289931
8	4/1/2014	2:30:06 PM	3.828	0.71	4.901	176.436		1.316548206	0.042997	1	1.795279	1.795278769	1.260951775	1.303949	1.336804002
9	4/1/2014	2:30:07 PM	3.899	0.763	5.219	187.884		-1.287566719	0.057488	-1	1.67564	-1.675640372	-1.176921232	-1.11943	-1.152247837
10	4/1/2014	2:30:08 PM	3.869	0.744	5.511	198.396		0.80095602	-0.18582	1	1.420565	1.420565218	0.997763837	0.811946	0.834515512
11	4/1/2014	2:30:09 PM	3.892	0.747	5.55	199.8		-0.248222819	0.090549	-1	0.413607	-0.413607199	-0.290505709	-0.19996	-0.20556198
12	4/1/2014	2:30:10 PM	3.883	0.782	5.527	198.972		-0.367161625	-0.21714	-1	1.10682	-1.106819852	-0.777398185	-0.99454	-1.025250172
13	4/1/2014	2:30:11 PM	3.858	0.744	5.57	200.52		0.83501023	0.016781	1	1.392159	1.392158735	0.977811947	0.994593	1.022239228
14	4/1/2014	2:30:12 PM	3.818	0.762	4.94	177.84		-0.637524775	0.115524	-1	1.559169	-1.559168826	-1.095114994	-0.97959	-1.008226928
15	4/1/2014	2:30:13 PM	3.893	0.793	5.277	189.972		-0.157217502	-0.28185	-1	0.891844	-0.891843504	-0.626405029	-0.90825	-0.937138873
16	4/1/2014	2:30:14 PM	3.812	0.745	5.493	197.748		0.912976887	0.096032	1	1.197781	1.197781418	0.841286952	0.937319	0.963447265
17	4/1/2014	2:30:15 PM	3.864	0.742	5.275	189.9		-0.519041614	0.293	-1	1.061322	-1.06132154	-0.745441489	-0.45244	-0.464946626
18	4/1/2014	2:30:16 PM	3.871	0.78	5.186	186.696		-0.46671988	-0.19988	-1	1.262737	-1.262736867	-0.886909778	-1.08679	-1.120166361
19	4/1/2014	2:30:17 PM	3.861	0.786	5.153	185.508		0.363022657	-0.25173	1	0.320662	0.320661943	0.225223655	-0.02651	-0.027332933
20	4/1/2014	2:30:18 PM	3.81	0.799	4.994	179.784		-0.083604405	-0.11202	-1	1.386645	-1.386644695	-0.973939044	-1.08596	-1.121054281
21	4/1/2014	2:30:19 PM	3.845	0.8	5.483	197.388		0.141894676	-0.08288	1	0.954365	0.954365349	0.670318561	0.587444	0.606478493
22	4/1/2014	2:30:20 PM	3.834	0.771	5.59	201.24		0.352299369	0.164222	1	0.182155	0.182154695	0.127940178	0.292162	0.300917171

Example of calculation

In this case, the example shows the calculation of the wind speed and wind direction at:

- Date : 1/4/2014
- Time : 2:30:02 PM

Direction part

Measurement data from recording are;

- o The resistance value of rotary potentiometer is 5.532 kΩ [P4]

For calculate the direction of wind is $\frac{[P4] \times 360}{10}$

$$\frac{[5.532] \times 360}{10} = 199.152^\circ \text{ [Q4]}$$

So, the direction of wind at 2:30:02 PM is 199.152°

Where 360 is the angle* in one round of rotary potentiometer and 10 is the maximum resistance value of rotary potentiometer or maximum range [0-10 kΩ].

*Remark: The angle is measured clockwise from a north base line.

Velocity part (x-axis)

Measurement data from recording are;

- The resistance value of linear potentiometer is 3.899 kΩ [C4]
- The resistance value of rotary potentiometer is 0.716 kΩ [D4]

- The distance of the spring moving is $x = \frac{[C4] \times 0.1}{10}$

$$x = \frac{[3.899] \times 0.1}{10}$$

$$x = 0.03899 \text{ m [E4]}$$

Where 0.1 is length of linear potentiometer and 10 is the maximum resistance value of linear potentiometer or maximum range [0-10 kΩ].

- The tension of spring can be found from $F_t = kx$

$$F_t = k[E4]$$

$$F_t = 1630 \times [0.3899]$$

$$F_t = 63.5537 \text{ N [F4]}$$

Where k is the spring constant (1630 N/m).

- The angle of rotary potentiometer is $\theta = \frac{[D4] \times 360}{10}$

$$\theta = \frac{[0.716] \times 360}{10}$$

$$\theta = 25.776^\circ \text{ [G4]}$$

Where 360 is the angle in one round of rotary potentiometer and 10 is the maximum resistance value of rotary potentiometer or maximum range [0-10 kΩ].

- The position of helium balloon in x-axis is $X = (L + R)\sin\theta$

$$X = (L + R)\sin[G4]$$

$$X = (38.25 + 1.5)\sin[25.776]$$

$$X = 17.285444 \text{ m [H4]}$$

Where L is the length of rope (38.25 m) and R is the radius of balloon (1.5 m).

- The position of helium balloon in y-axis is $Y = \sqrt{40^2 - X^2}$

$$Y = \sqrt{40^2 - [H4]^2}$$

$$Y = \sqrt{40^2 - [17.285444]^2}$$

$$Y = 36.072336 \text{ m [I4]}$$

Where 40 is the maximum point of the position of the helium balloon can be.

- The acceleration of the helium balloon in the x-axis is $\ddot{x} = \frac{x(t) - 2x(t - \Delta t) + x(t - 2\Delta t)}{(\Delta t)^2}$

$$\ddot{x} = \frac{[H4] - 2[H3] + [H2]}{(\Delta t)^2}$$

$$\ddot{x} = \frac{[17.285444] - 2[17.3079312] + [18.5781338]}{(1)^2}$$

$$\ddot{x} = 1.247715448 \text{ m/s}^2 \text{ [J4]}$$

Where $x(t)$, $x(t - \Delta t)$, and $x(t - 2\Delta t)$ are the positions of the helium balloon at times t , $(t - \Delta t)$, and $(t - 2\Delta t)$, respectively and Δt is the sampling time (1 s).

- The velocity of the helium balloon is $v_b = \frac{x(t) - x(t - 2\Delta t)}{2(\Delta t)}$

$$v_b = \frac{[H4] - [H2]}{2(\Delta t)}$$

$$v_b = \frac{[17.285444] - [18.5781338]}{2(1)}$$

$$v_b = -0.64634492 \text{ m/s [K4]}$$

- The drag force is $F_d = m\ddot{x} + F_t \sin\theta$

$$F_d = m[J4] + [F4] \sin[G4]$$

$$F_d = 2.354[1.247715448] + [63.5537] \sin[25.776]$$

$$F_d = 30.5737 \text{ N}$$

Where m is mass of balloon without air or gas (2.354 kg).

- The wind speed is $v = \sqrt{\frac{F_d}{0.5\rho c_d A}} + v_b$

$$v = \sqrt{\frac{F_d}{0.5\rho c_d A}} + [K4]$$

$$v = \sqrt{\frac{30.5737}{0.5(1.2203)(0.47)(7.068583)}} + [-0.64634492]$$

$$v = 3.237309462 \text{ m/s [L4]}$$

Where ρ is the density of air (1.2203 kg/m^3), c_d is the drag coefficient (0.47) and A is cross-sectional area of the helium balloon (7.068583).

- Apply power laws to wind speed $v_d = v\left(\frac{y_d}{y}\right)^\alpha$

$$v_d = [L4]\left(\frac{y_d}{[L4]}\right)^\alpha$$

$$v_d = [3.237309462]\left(\frac{40}{[36.072336]}\right)^{0.245}$$

$$v_d = 3.320329766 \text{ m/s [M4]}$$

So, the direction of speed in x-axis at 2:30:02 PM is 3.320329766 m/s

Where y_d is a desired height (40 m) and α is the ground friction coefficient (0.245).

Velocity part (y-axis)

- The acceleration of the helium balloon in the y-axis is $\ddot{y} = \frac{y(t)-2y(t-\Delta t)+y(t-2\Delta t)}{(\Delta t)^2}$

$$\ddot{y} = \frac{[I4]-2[I3]+[I2]}{(\Delta t)^2}$$

$$\ddot{y} = \frac{[36.072336]-2[36.0615518]+[35.423906]}{(1)^2}$$

$$\ddot{y} = -0.62686 \text{ m/s}^2 \text{ [S4]}$$

- The velocity of the helium balloon is $v_{b_y} = \frac{y(t)-y(t-2\Delta t)}{2(\Delta t)}$

$$v_{b_y} = \frac{[I4]-[I2]}{2(\Delta t)}$$

$$v_{b_y} = \frac{[36.072336]-[35.423906]}{2(1)}$$

$$v_{b_y} = 0.324216 \text{ m/s [T4]}$$

- The drag force is $F_{d_y} = m\ddot{y} + mg - F_b + F_g + F_t \cos\theta$

$$F_{d_y} = m[J4] + mg - F_b + F_g + [F4] \cos[G4]$$

$$F_{d_y} = 2.354[1.247715448] + 2.354(9.81) - (169.238) + 89.97922 + [63.5537] \cos[25.776]$$

$$F_{d_y} = -0.41151 \text{ N [V4]}$$

Where g is the gravitational acceleration (9.81 m/s^2), F_b is the buoyancy force (169.238 N) and F_g is gas weight (89.97922).

- The wind speed is $v_y = \sqrt{\frac{F_{dy}}{0.5\rho c_d A}} + v_{by}$

$$v_y = \sqrt{\frac{F_{dy}}{0.5\rho c_d A}} + [T4]$$

$$v_y = \sqrt{\frac{0.41151}{0.5(1.2203)(0.47)(7.068583)}} + [0.324216]$$

$$v_y = 0.12635 \text{ m/s [Y4]}$$

- Apply power laws to wind speed $v_d = v\left(\frac{y_d}{y}\right)^\alpha$

$$v_d = [Z4]\left(\frac{y_d}{[I4]}\right)^\alpha$$

$$v_d = [0.12635]\left(\frac{40}{[36.072336]}\right)^{0.245}$$

$$v_d = 0.12959 \text{ m/s [Z4]}$$

So, the direction of speed in y-axis at 2:30:02 PM is 0.12959 m/s

Appendix C

Simulation

In this study, MATLAB software is used to simulate the moving of helium balloon to measure the wind direction and wind speed.

The equations were written in M-file to use in simulation of MATLAB software.

Simulation of wind direction

```

m=0.2; % m is mass of swing arm
L=3; % L is length of rope
Lp=0.1; % Lp is length of rope in top view
T=40; % T is tension force of rope
rsa=0.2; % rsa is length of swing arm
delt=0.0005; % delt is change in time
ctsa=0; % ctsa is angle of swing arm
ctw=pi/6; % ctw is angle of wind
I=m*(rsa^2)/3; % I is moment of inertia of swing arm
D=0; % D is damping factor
ctsad=0; % ctsad is angular velocity of swing arm
xa=rsa; % xa is location of coordinate x at point a
ya=0; % ya is location of coordinate y at point a

for i=1:10000;

ctsadd=(((T*(rsa*cos(ctsa))*(Lp*cos(ctw))*(tan(ctw)-tan(ctsa))/L)-ctsad*D))/I;
% ctsadd is the angular acceleration of the
rotating arm about the y axis at equation (3.3)
ctsadtdt=ctsad+ctsadd*delt; % ctsadtdt is velocity of swing arm at time
(t + Δt)
ctsatdt=ctsa+ctsad*delt; % ctsatdt is angle of swing arm at time (t + Δt)

```

```

ctsad=ctsadtdt;
ctsa=ctsatdt;

st(i)=delt*i;
sctsa(i)=ctsa;
end

plot(st,sctsa,'B');

```

Simulation of wind speed

```

v=3; % v is velocity of wind
cd=0.47; % cd is drag coefficient
dair=1.14; % dair is density of air
dhe=0.1785; % dhe is density of helium
m=0.056; % m is mass of balloon
g=9.81; % g is gravitational acceleration
L=3; % sL is length of rope
r=1; % r is radius of balloon
t=0; % t is time
A=pi*(r^2); % A is area surface of balloon
V=pi*4/3*r^3; % V is volume of balloon
Fg=dhe*V*g; % Fg is gas weight
Fb=dair*V*g; % Fb is buoyancy force of balloon
T=Fb-Fg-m*g; % T is tension force of rope
delt=0.0005; % delt is change in time
xpt=0; % xpt is velocity of balloon in x-axis
ytmtdt=L+r; % ytmtdt is location of balloon in y-axis at time (t - Δt)
yptmtdt=0; % yptmtdt is velocity of balloon at time (t - Δt)
yt=L+r; % yt is location of balloon in y-axis at time (t)
xt=0; % xt is location of balloon in x-axis at time (t)

```



```

j=1; % j is change in time for measuring simulation
m_xtmdt=0; % m_xtmdt is location of balloon in x-axis at time
(t - Δt) for measuring simulation
m_xtm2dt=0; % m_xtm2dt is location of balloon in x-axis at time
(t - 2Δt) for measuring simulation

for i=1:10000
if i==1000
v=2;
end
if i==2700
v=1;
end
if i==4000
v=0;
end
if i==4600
v=-1;
end
if i==6700
v=-2;
end
if i==7000
v=-3;
end
if i==8600
v=-1;
end

Fw=sign(v)*(0.5*dair*cd*A*(v-xpt)^2); %Fw is drag force at equation (3.5)
gm=atan(xt/(L+r)); % gm is swing angle between the cord and
the vertical line at equation (3.11)

```

```

ax=((Fw-T*sin(gm))/m);           % ax is acceleration in the x axis at
                                  equation (3.7)

xptdt=xpt+ax*delt;              % xptdt is velocity of balloon in x-axis at
                                  time (t + Δt)

xtdt=xt+xpt*delt;              % xtdt is location of balloon in x- axis at
                                  time (t + Δt)

yt=sqrt(((L+r)^2)-xt^2);

ypt=-xt*xpt/yt;                % ypt is velocity of balloon in y-axis
ay=(-xpt-xt*ax-ypt)/yt;        % ay is acceleration in the y axis at
                                  equation (3.6)

T=(Fb-m*g-Fg-m*ay)/cos(gm);

xpt=xptdt;
xt=xtdt;

st(i)=delt*i;
sy(i)=yt;
sx(i)=xt;
sT(i)=T;
sax(i)=ax;
say(i)=ay;
sgm(i)=gm;
sFw(i)=Fw;
sxpt(i)=xpt;
sv(i)=v;

```

```

if i==j*100
m_delt=100*delt;

m_ax=(xt-2*m_xtmdt+m_xtm2dt)/(m_delt^2);
% m_ax is acceleration in the x axis
% formeasuring simulation

m_xpt=(xt-m_xtmdt)/m_delt; % m_xpt is velocity of balloon in x-axis
% for measuring simulation

m_v=sign(v)*sqrt(2*abs((T*sin(gm)+m*m_ax))/(dair*cd*A))+m_xpt;
% m_v is velocity of wind for measuring
% simulation

m_xtm2dt=m_xtmdt; % m_xtm2dt is location of balloon in x-
% axis at time (t - 2Δt)

m_xtmdt=xt; % m_xtmdt is location of balloon in x-
% axis at time (t - Δt)

sm_ax(j)=m_ax;
stj(j)=m_delt*j;
sm_xpt(j)=m_xpt;
sm_v(j)=m_v;
j=j+1;
end
end

plot(st,sv,'B');
hold on
plot(stj,sm_v,'R');
hold off

```